On Demand Deployment of UAV Base Stations in Wireless Communication Networks

Mohamed Hydher Mohamed Hassaan

198134K

Thesis submitted in partial fulfilment of the requirements for the degree Master of Science by research.

Department of Electronic and Telecommunication Engineering

University of Moratuwa
Sri Lanka

April 2022

Declaration

I declare that this is my own work and this thesis/dissertation does not incorporate without acknowledgement any material previously submitted for a Degree or Diploma in any other University or institute of higher learning and to the best of my knowledge and belief it does not contain any material previously published or written by another person except where the acknowledgement is made in the text.

Also, I hereby grant to University of Moratuwa the non-exclusive right to reproduce and distribute my thesis/dissertation, in whole or in part in print, electronic or other medium. I retain the right to use this content in whole or part in future works (such as articles or books).

Signature: Date:

The above candidate has carried out research for the Masters thesis/dissertation under my supervision.

Signature of the supervisors:

1. Date:

2. Date:

3. Date:

Abstract

Unmanned aerial vehicles (UAVs)-assisted communication systems are considered a promising technology in diverse verticals. The objective of this research is to study on demand deployment of UAVs in special applications. We analyze the multi-UAV deployment in two different scenarios.

First, we analyze the deployment of UAVs as an aerial base stations (ABSs) to provide cellular coverage to isolated users. The main contributions of this study includes a less complex approach to optimally position the UAVs and assigning user equipment (UE) to each ABS, such that the total spectral efficiency (TSE) of the network is maximized, while maintaining a minimum QoS requirement for the UEs. The main advantage of the proposed approach is that it only requires the knowledge of UE and ABS locations and statistical channel state information. We propose two approaches with common and diverse altitude selection. Both approaches lead up to approximately 8-fold energy savings compared to ABS placement using a naive exhaustive search.

Second, we have investigated the deployment of UAVs in wireless sensor network (WSN) systems. Considering the energy-constrained nature of the WSN, we have proposed a multi-UAV deployment algorithm that minimizes the maximum power transmitted among the sensor nodes (SN) for given data rate and altitude constraints. The problem is divided into three subproblems in order to reduce the complexity. Each subproblem is optimized by fixing other parameters as constant. Finally, we proposed a joint optimization algorithm that combines the approaches of all three subproblems. In the joint optimization, the first and second subproblems are iteratively solved together while third subproblem is solved independently for each UAV. Moreover, the joint optimization gives the minimum number of UAVs required to serve all the SNs with the given constraints. The results indicate a significant performance gain compared to the benchmark methods in terms of the number of iterations for convergence, maximum transmission power requirement and the minimum number of UAV requirements.

Acknowledgements

First and foremost, I would like to acknowledge and give my warmest thanks to my supervisors Dr. K.T. Hemachandra, Dr. T.N. Samarasinghe and Prof. D.N.K. Jayakody who made this work possible. Their guidance and advice carried me through all the stages of my project. This journey help me to shape my technical approaches in several angles.

I would like to extend my thanks to all the colleagues who worked with me at centre for telecommunication research (CTR) for providing your support in various ways. Also, I would like to give a special thank to my family as a whole for their continuous support and understanding when undertaking my research and writing my project.

Contents

List of Figures

List of Tables

Chapter 1

Introduction

1.1 UAV and wireless communication

Unmanned aerial vehicles (UAVs), generally referred to as drones, have a diverse range of use cases. The usage of UAVs is exponentially growing and has become an inevitable technology in various fields [1, 2]. UAVs' initial research and experimentation date back to the interwar period, when the British army developed radio-controlled planes to serve as targets in military exercises. However, UAV applications have been underutilized for a long time due to various problems with cost-effective design, accurate and sensitive control, energy-efficient processing and durable batteries [3]. Continuous advancements in payload capacity, complex control mechanisms, energy-efficient processing, and increment in flight-time endurance have paved the way for many other promising UAV-assisted applications. The applications include but are not limited to agriculture, patrolling, mapping & surveying, search & rescue, disaster management and entertainment.

The current trend portrays increasing interest in UAV-assisted applications in diverse verticals. This growth is expected to be the key enabler of accomplishing the milestones of a smart environment [1, 2]. In all of the above-discussed applications, the UAVs are deployed as cellular-connected UAVs, where they act as an aerial user equipment, which is controlled by the respective cellular infrastructure. Therefore, a smooth, stable, and reliable communication infrastructure is essential to make these applications feasible. The wireless communication sector is constantly improving the factors that allow UAVs to capitalize on their potential as a smart environment enabler. The control commands and overhead

requirements by UAVs require reliable and low latency communication and are fulfilled by ultra-reliable low latency communications (URLLC), which is one of the primary use cases of fifth-generation (5G) new radio (NR) [4]. On the other hand, data payload delivery requirements are jointly fulfilled by the other two use cases of 5G NR; namely, enhanced mobile broadband (eMBB) and massive machine type communication (mMTC) [5].

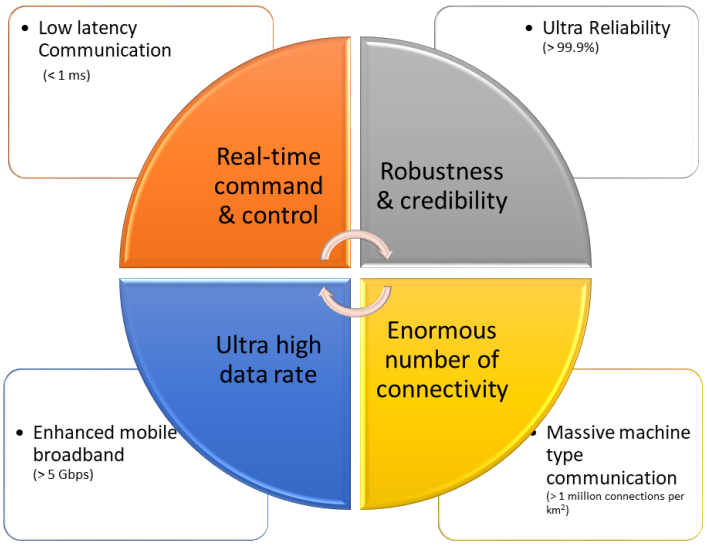

Fig. 1.1: Requirements of UAV-assisted applications and the relevant use case of 5G and beyond networks that aid the demand

On the other hand, wireless communications have drastically evolved over the past decades, from pure voice transmissions to rich multimedia content and other data. Along with this, the popularity of cloud computing and smartphone usage creates tremendous data traffic in wireless communication networks. Currently, the 5G cellular networks are being deployed globally. Similar to wireless standards support cellular-connected UAV applications, the UAVs are deployed to support and enhance various applications in wireless networks, which is generally referred to as UAV-assisted communication

1.2 UAV-assisted wireless communication

UAV-assisted wireless communication is generally studied for two cases, where the UAV acts as an aerial base station [6], or an aerial relay station [7]. Potential

applications of aerial base stations are supporting the overloaded terrestrial base stations (BSs), providing on-demand coverage in no coverage areas for special occasions, and reconstructing temporary coverage in a natural disaster or an emergency situation [1, 2, 8]. The UAVs are deployed as aerial relay stations where the channel link between the source and the destination is unavailable or too weak for successful communication [7, 9, 10]. On the other hand, there is an increasing interest in utilizing UAVs for data gathering applications where they collect the data from diverse geographic regions around a city or a remote area and deliver it to a central station for analysis [1]. Notably, data collection of UAVs is getting more attention in wireless sensor network (WSN) systems. In conclusion, UAV-assisted communication can be divided into three general areas, namely,

1. UAV-assisted ubiquitous coverage,
2. UAV-assisted relaying, and
3. UAV-assisted data dissemination/collection.

1.2.1 UAV-assisted ubiquitous coverage.

UAVs can be deployed as aerial base stations that improve wireless connectivity and provide multi-access edge computing (MEC) services. Providing uninterrupted and reliable coverage is a key feature of future wireless communications. UAVs can be deployed in diverse network systems to address this requirement. Remote controllability and the mobility of a UAV make it possible to deploy anywhere, irrespective of the terrain conditions. Moreover, UAVs are a promising candidate for on-demand deployment due to the low cost of deployment and simple infrastructure requirements. Furthermore, it can improve the signal quality due to the ability to hover at appropriate altitudes to establish a strong line of sight (LoS) links with the ground users.

Profited from these benefits, UAV-assisted systems have great potential to provide edge computing services and ubiquitous coverage associated with ground or satellite systems. Application scenario of UAV as aerial base station can be categorized as,

- **Emergency scenarios**
  Natural disasters, such as volcanic eruptions, typhoons, floods, cyclones,

earthquakes and tsunamis, can destroy terrestrial infrastructure. It is vital to have a communication system enabled to gather and process data from sensors and emergency workers for conducting emergency rescues. Here, the UAV is capable of temporarily enabling the communication infrastructure.

- **Hotspot events**
  It is difficult to maintain the quality of experience (QoE) standards for a massive number of users in hotspot areas like athletic events, football fields, political rallies and traffic jams solely through the terrestrial network. The integration of UAVs has enormous potential for addressing the vital increase in communication and processing requirements. As a result, UAV-assisted networks could help improve user experiences in hotspot locations.

- **Remote areas**
  Establishing a fully-fledged terrestrial communication infrastructure in remote areas is not cost-effective. However, there could be requirements to provide coverage for rural areas or areas that do not have terrestrial infrastructure due to special temporary events or data collection requirements. In these situations, UAVs can be deployed to provide on-demand coverage.

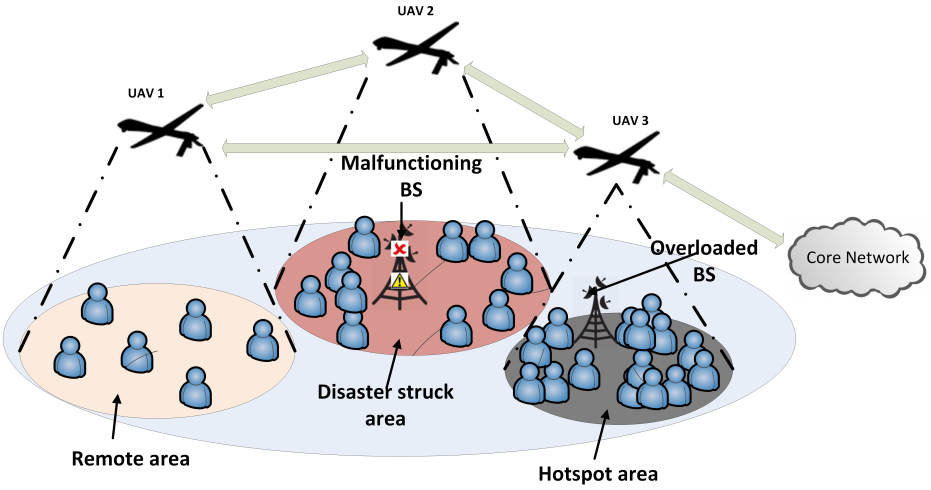

Fig. 1.2: Application scenarios of UAV as aerial base station

1.2.2 UAV-assisted relaying.

Extending or strengthening the wireless coverage is a key application of relay nodes. The UAVs also can be used as aerial relays in an instance where the ob-

stacle completely blocks the propagation path between the source to destination or the path experiences a deep fade. UAVs can act as a relay to establish the obstructed link or minimize the fading by strong LoS propagation. Aerial relaying has numerous advantages over a standard fixed relay system thanks to the flexible and on-demand nature of UAVs.

1.2.3 UAV-assisted data dissemination/collection.

On the other hand, there is an increasing interest in utilizing UAVs for data gathering applications where they collect the data from diverse geographic regions around a city or remote area and deliver it to a central station for analysis [1]. Notably, data collection of UAVs is getting more attention in wireless sensor network (WSN) systems.

The wireless sensors enabled broad and diverse utilization in locations where wired sensors are not feasible to be deployed. As WSN can be remotely controlled, it can cover a vast geographical area. It can be deployed to accumulate information from large agricultural fields, forests, heritage lands, etc. There are several UAV applications in WSN systems, but not limited to, as follows. First, It can help to collect data from remote areas where deploying a ground station (GS) is not feasible and cost-effective [10]. Second, as these WSNs are deployed in a huge geographical area in large quantities, it is not feasible to recharge them individually. Thus, it can be recharged through wireless power transfer (WPT) enabled UAV, which is a feasible and promising solution as the battery capacity of WSNs is not too high [7]. Third, it can be deployed as a temporary data collector where the dedicated GS malfunctions due to a disaster or other technical problems. Our proposed model is applicable in collecting data from remote areas and as well as it can be utilized as a temporary data collector in emergencies.

Utilizing UAVs for data collection tasks can bring several benefits but is not limited to as follows. First, the ability to adjust the altitude allows enabling strong LoS propagation that will strengthen the channel. Second, UAVs not only possess data transmission but data computation, caching, and processing capacities. They can directly receive the data from the nodes, do the respective operation, carry stored data, and offload it to the GS. This ability to store and

forward the data creates a new cooperative communication protocol as store-and-forward (SF) relaying [12]. Third, simple infrastructure requirements and ease of deployment make it suitable for on-demand deployment. Fourth, UAVs are maneuverable. They can freely adjust their aerial stopping locations to improve the system's performance. Fifth, it can utilize simultaneous wireless information and power transfer (SWIPT) techniques to recharge the SNs while collecting data.

1.3 Challenges in UAV-assisted communication

Compared to terrestrial communication, several challenges are involved in facilitating the UAV-assisted communication network. The higher mobility demands complex control mechanisms [1] and effective trajectory planning, while on-demand deployment requires self-organizing network (SON) capability [13]. Furthermore, the higher probability of LoS links increases the co-channel interference (CCI). Thus, the control algorithm plays a crucial role in such a network, as it should focus on several aspects that ensure the system's proper functioning. These include radio resource management, interference management, channel estimation and prediction, placement, user association, energy efficiency, and trajectory planning. Therefore, significant research has recently been focused on the intelligent planning of UAV networks. Below we have mentioned some of the challenges involved in UAV-assisted communication.

- **UAV placement and path planning**

  Maneuverability is an essential advantage that UAVs provide when using UAV-assisted communication systems. In terrestrial infrastructure, deployment and planning are done through a long-term behavior of data demand and the area's geological structure. However, deployment and path planning of UAV aerial devices should be done considering the real-time information. Initially, the objective of the network should be identified with the relevant constraints. Then the appropriate algorithm should be adopted, or a customized algorithm should be developed to decide the deployment and path planning. In the literature, both centralized and disseminated algorithms are considered for deployment. Considering the wing type, the path planning of the UAV differs. Those are discrete and continuous trajectories

in the spatial realm. It is necessary to have a continuous trajectory for fixed-wing UAVs as it is essential to keep a minimum speed to maintain the respective altitude. On the other hand, Rotary-wing UAVs can have both discrete and continuous trajectories as they can standstill in the air. In a disaster scenario or an emergency application, rotary-wing UAVs have more benefits than fixed-wing UAVs.

- **Energy efficiency**

  Energy efficiency is a crucial factor in extending the UAVs' battery life or hovering time as UAVs are powered by energy-constrained power resources. In a UAV-assisted communication system, the energy is consumed for mobility and data transferring. Comparably, mobility needs more power than transmission. Thus, it significantly impacts the energy efficiency of the system. Therefore, a fundamental trade-off exists between energy consumption and the quality of service, which is most of the time measured in relation to data rates provided.

- **User association and moving cells**

  In a terrestrial system, user association is done by defining the cell boundaries by analyzing the RF footprint. The cell boundaries are defined through a long-term statistical interpretation of data request trends and the area's geological structure. However, the UAV aerial base station can not have a determined cell structure. It has the notion of a moving cell. In the moving cell concept, the user association decision should be based on the instantaneous or predicted value. Matching algorithms are the ones mostly used to tackle User association. Initially, the cost weight of the system should be identified. Cost features can be energy consumption, latency, data rate, etc. After that, the cost value will be weighted for each UAV-user link, where the respective matching algorithm can be used to solve the user association problem.

- **Air-to-ground channel modelling**

  The data collection link represents the communication between the user and the UAV. It is often referred to as ground-to-air (GTA) link, which almost has the same characteristics as its reciprocal air-to-ground (ATG) link. The ATG channel could experience both LoS and non-LoS (NLoS) propagation depending on the position of the aerial device, ground device and environmental parameters. To exactly calculate the contribution of LoS and NLoS propagation in ATG channel gain, we should have accurate and precise information related to the geometrical structure of that particular environment. As we do not have access to such information, we have to think of an effective alternative method to characterize the LoS and the NLoS contribution in the ATG channel.

  There are no universally affirmed channel models to characterize the ATG channel. However, there are four kinds of models that have been used to characterize the GTA channels in the current literature. First, the channel model, which utilizes the exact geometrical structure of the environment and the reflective nature of the wavefront. Second, the empirical measurements based channel models. Third, pure LoS propagation which is often modeled using the free-space path loss model. Finally, probabilistic information-based LoS characterization is used to model the contribution of LoS and NLoS propagation.

1.4 Objectives and Scope

The objective of this research is to study the challenges involved in UAV deployment for diverse applications, and propose effective algorithms for UAV placement. The study is divided into two phases.

Phase-I- Study the deployment of UAVs as ABSs, which provide ubiquitous coverage to the ground users, and propose an effective algorithm for UAV ABS placement. This phase mainly deals with the following tasks.

- Study the challenges involved in deploying UAVs as ABSs.

- Identify the crucial performance and the constraints of ABS which should be ensured through the deployment.
- Investigate the drawbacks of the approaches proposed in the current literature.
- Propose an algorithm that addresses the identified constraints and drawbacks in existing work.

Phase-II- Study the deployment of UAVs as a data collector, which collects data from the sensor nodes and forward it to a ground station. For this scenario, propose an effective algorithm for deploying UAVs as data collectors.

- Study the challenges involved in deploying UAVs as data collectors.
- Identify the crucial performance and the constraints in the WSN system and deployment of UAV as a data collector
- Investigate the drawbacks of the approaches proposed in the current literature.
- Propose a UAV placement algorithm that addresses the identified constraints and drawbacks of existing work.

1.5 Organization of the Thesis

The remainder of this thesis is organized as follows. Chapter 2 discusses the related works and provides the motivation for both works that we have addressed in this thesis. Chapter 3 discusses our initial work, which focuses on deploying UAVs as ABS to maximize the system's spectral efficiency. Similarly, chapter 4 discusses our second work, which is focused on UAV deployment for energy-efficient WSN systems. Finally, the thesis is wrapped by providing some future directions.

1.6 Publications

Below are the publications that arose through this work,

- H. Hydher, D. N. K. Jayakody, K. T. Hemachandra, and T. Samarasinghe, "Intelligent UAV deployment for a disaster-resilient wireless network," *Sensors*, vol. 20, no. 21, p. 6140, Oct. 2020.

- H. Hydher, D. Jayakody, K. Hemachandra and T. Samarasinghe, " UAV Deployment for Data Collection in Energy Constrained WSN System" *in Proc. IEEE International Conference on Computer Communications (INFOCOM), Workshop on Artificial Intelligence (AI) and Blockchain-Enabled Secure and Privacy-Preserving Air and Ground Smart Vehicular Networks*, 2022.

Chapter 2

Related Works and Motivation

One of the key advantages of UAVs in the application of wireless communication is mobility. It arises the challenges related to UAV deployment. Several factors must be considered in UAV deployment in UAV-assisted communication to ensure the system's performance. Such as resource management, coverage region, interference management, channel prediction, deployment, user assignment, path planning, energy efficiency, etc.

2.1 Deployment Approaches Proposed for UAV-Assisted Communication

2.1.1 UAV as an aerial base station

Several works in the literature address the various challenges related to UAV deployment. Initially, we did a background study to analyze the deployment approaches proposed in the current literature to provide ubiquitous coverage. It is summarized in Table 2.1.1.

Table 2.1: Some general deployment approaches proposed in the current literature.

Reference	**Objective**	**Methodology/ Algorithm**	**Remarks**
[14]	Optimal altitude for maximum coverage region	Model the signal loss as a function of altitude and find the critical point to minimize the function	Simplified probability of LoS calculation
[15]	Optimal position of BS to fit the area of interest considering coverage circles.	Circle packing theory	LoS effect on small scale fading is not considered
[16]	Optimal placement for Energy-Efficient Maximal Coverage	Circle packing theory	Interference is totally neglected
[17]	Optimal placement for higher data rate	Genetic algorithm	Interference is totally neglected
[18]	Cognitive adaptation network to provide connectivity between IoT devices with minimal ABS	Feedback based iterative algorithm	LoS is not considered in any cases and leads unrealistic channel model for an ABS

Continued on next page

Table 2.1 – *Continued from previous page*

Reference	**Objective**	**Methodology/ Algorithm**	**Remarks**
[19]	Adjusting the UAV heading to maximize the approximate ergodic sum rate of the uplink channel	Centralized algorithm which guarantees optimal solution	Interference is totally neglected
[20]	Maximize the system throughput	Develop an algorithm for dynamically adjust the movement	Absolute LoS assumption, Interference is not considered.
[21]	Improve transmission efficiency and maximize system throughput	Adaptive weighted coordinate axes algorithm	Interference is totally neglected
[22]	Minimum number of drone-BSs and their 3D placement so that all the users are served	Particle swarm optimization	Requires high computational power

After the initial background study, we identified some drawbacks in the current literature. Given those, we further analyzed the similar works in the literature and sculptured our system model and our approach such that it overcomes the identified drawbacks. Table 2.2 briefly describes the drawbacks that we identified in the current literature and also how it is addressed through our proposed system model.

Table 2.2: Limitation in the existing works and the proposed way to overcome

Reference	**Limitation in their system model**	**The way our system model overcomes the limitation**
[16, 20, 23, 24, 25]	In these approaches, they have not considered the interference between the UAVs when considering the signal quality.	In our approach, we have considered the interference from each and every other UAVs (co-channel interference).
[20, 24, 25, 26]	These approaches do not consider the combined effect of LoS and NLoS on signal quality.	In our approach, we consider the effect of LoS and NLoS on signal quality.
[16, 20, 23, 24, 25, 26]	These approaches do consider the effect of LoS and NLoS in large-scale path loss effect, but it does not consider the effect in small-scale fading.	In our approach, we consider the LoS and NLoS effect in small scale fading.
[15, 16, 24]	These approaches use a coverage disc-based approach to decide which UE will be covered by which UAV (user assignment). It is not feasible if we take interference into account. In [15], they have an assumption of equal average interference throughout the circumference. It is not feasible in practical scenarios. Also, the disc assumption is valid if we only consider average pathloss. If we include shadowing and small-scale fading, the shape will not be predictable.	In our approach, user assignment is done through the calculated channel link quality using statistical channel state information (CSI).

Continued on next page

Table 2.2 – *Continued from previous page*

Reference	**Limitation in their system model**	**The way our system model overcomes the limitation**
[24, 25, 26]	These works have not considered the impact of altitude in the performance analysis.	In our works, we have set a minimum and maximum altitude for the UAV where the UAV can take any altitude in between them. Also, we have considered the impact of altitude on the probability of LoS and the pathloss.
[15, 20]	Moreover, these works have considered a fixed altitude for the performance analysis.	
[27]	They have included most of the aspects. However, they have not considered the effect of LoS in small-scale fading. They have assumed Rayleigh fading assumption for both LoS and NLoS propagation.	In our approach, we consider the effect of LoS in small-scale fading as well. For LoS we consider the rician fading assumption and for NLoS rayleigh fading assumption.
[15, 17, 19, 20, 27]	These approaches require knowledge of perfect channel state information of all users in each and every ABS. Also, in some approaches, it takes a time average of CSI on the UE's end prior to feedback to the ABSs. This will also be time-consuming. This is one of the major drawbacks in the current literature.	We are proposing an approach to utilize statistical CSI of the channel to overcome this drawback. The detailed discussion of this concern is in section 3.3.

Continued on next page

Table 2.2 – *Continued from previous page*

Reference	**Limitation in their system model**	**The way our system model overcomes the limitation**
[15, 16, 17, 18, 19, 20, 21, 22, 23, 25, 26, 27]	In these works, they have not included the energy constraint for maneuvering. The energy required for maneuvering is relatively high, which can not be neglected. This is also a major drawback in the constraints of current literature.	We have included the constraints on the energy required for UAV maneuvering in our system model.

All things considered, our initial work is focused on the problem of optimal placement of the UAVs as ABSs to enable network connectivity for the users in an emergency. It is thoroughly discussed in chapter 3.

2.1.2 Energy efficiency in UAV-assisted communication system

In the initial work, we focused on positioning the UAV to maximize the total spectral efficiency of the system. At the same time, it consumes less energy for mobility than the sequential approaches proposed in the existing literature. However, considering the limited energy nature of the UAV-assisted systems, overall energy efficiency is crucial for such a system. Therefore, in the next phase, we focus on energy efficiency in a UAV-assisted communication system.

We did a background study to analyze the deployment approaches proposed in the current literature, which focus on energy efficiency in UAV-assisted communication. It is summarized in Table 2.3.

Table 2.3: Works Related to Energy Efficient UAV-assisted Communication System

Work	Objective	Constraints	Methodology/ Algorithm
[28]	Energy efficiency for the secrecy capacity is maximized by optimizing the transmit powers and the trajectory of the UAV through a joint optimization.	Maximum transmit power, Maximum UAV Speed, Completion of the complete cycle of the trajectory	Block coordinate descent (BCD) and Dinkelbach method is used in a recursive algorithm to obtain a suboptimal solution by combining successive convex approximation (SCA) techniques.
[29]	Deployment of access point (AP) and fusion centers such that the total power consumption of sensor node is decreased.	Maximum transmit power	Modified Lloyd algorithm
[30]	Maximize the UAV's energy efficiency for secrecy communication by optimizing UAV's trajectory, flight velocity design, User scheduling and power allocation.	Maximum tolerable signal-to-noise ratio (SNR) leakage, minimum data rate requirement	Two subsequent optimization approaches. First, for feasible UAV's trajectory and flight velocity, optimize the user scheduling and the transmit power allocation. Then, for feasible user scheduling and transmit power allocation optimize the UAV's trajectory and flight velocity.

Continued on next page

Table 2.3 – *Continued from previous page*

Work	**Objective**	**Constraints**	**Methodology/ Algorithm**
[31]	Energy efficiency of the UAV is maximized by optimizing its trajectory.	Mobility constraints of the UAV.	Iterative approach that follows SCA technique and Dinkelbach's algorithm
[32]	Minimizing the total energy consumption of a UAV deployment in a straight road.	Minimum data rate, maximum delay.	BCD
[33]	Maximize the energy-efficient of UAV relaying by jointly optimizing UAV's acceleration, trajectory and flying speed and also the transmit power of UAV and BS.	UAV mobility constraints, UAV and BS transmit power constraint.	First, solve the transmit power of BS and UAV, and speed for a given UAV location and acceleration. Second, using the suboptimal UAV location and acceleration in the previous subproblem, optimize the transmit power of BS and UAV and speed. Iterate it until the convergence.
[34]	Optimal deployment considering minimizing the number of UAVs per hour of service.	Coverage and QoS constraints.	Genetic Algorithm and Particle Swarm Optimization.

Continued on next page

Table 2.3 – *Continued from previous page*

Work	**Objective**	**Constraints**	**Methodology/ Algorithm**
[35]	Maximizing energy efficiency in UAV communication via optimizing UAV and BS transmit power; UAV trajectory, acceleration, and flying speed.	UAV mobility and maximum transmit power constraints	SCA techniques and Dinkelbach's algorithm.
[36]	Maximizing the sum of logarithmic rates by optimizing the position of the UAV.	Maximum coverage radius and minimum and maximum UAV altitude	Particle Swarm Optimization.
[37]	Maximize energy efficiency by designing the transmit power allocation, user scheduling, UAV's flight velocity and trajectory.	Maximum tolerable leakage signal-to-interference plus-noise ratio (SINR) to eavesdroppers and the minimum individual user data rate requirement.	SCA and the Dinkelbach's method.
[38]	Minimize the sum energy consumption of IoT nodes by optimizing UAV position and the user association.	Node association constraints.	K-means clustering and cutting plane method

Continued on next page

Table 2.3 – *Continued from previous page*

Work	**Objective**	**Constraints**	**Methodology/ Algorithm**
[39]	Scenario 1: minimize the time that is needed to complete data transmission; Scenario 2: power allocation and the UAV's position are jointly optimized to maximize the size of data that can be transmitted.	Total power constraint	Customized Algorithm which includes bisection method, Newton-Raphson method and Golden-section method.
[40]	Optimal trade-off between the ground transmitter and UAV power consumption.	Minimum transmit power constraint on ground and UAV transmitter	Analytical approach given the probability density function of the position of ground transmitter and ground receiver.
[41]	Maximize the secrecy energy efficiency (ratio between secrecy capacity and energy efficiency) by optimizing the communication schedule, power allocation, and UAV trajectory	Minimum transmit power constraint on ground and UAV transmitter	Iteratively solving the subproblem through convex optimization and SCA.

Below we mention some extracted points after analyzing the above works,

- No works have included transmitting power allocation considering the system's energy efficiency.

- In general, the energy efficiency of a UAV network is defined as

$$Energy \;\; Efficiency(EE) = \frac{Spectral \;\; Efficiency \;\; or \;\; Capacity}{Energy \;\; Consumption(Mechanical \;\; Movement)}$$

- Considering the above definition of EE, transmit power is treated as an optimization variable to achieve higher spectral efficiency and increase EE in most works. However, the energy consumption for transmission is neglected.

- Considering the non-convexity of the EE maximization problem concerning user scheduling, trajectory and transmit power, most of the works propose dividing them into subproblems and solving them using iterative approaches.

- Most of the works assume pure LoS propagation is always possible in the air-to-ground channel link to avoid the complexity of altitude adjustment. Also, the simple free-space path loss is adopted to calculate the channel gain related to each link.

Although the transmit power is negligible compared to the power required for propeller movement. it significantly affects the energy efficiency of the uplink communication. Therefore, we further analyzed the works that focus on uplink communication. It is summarized in Table 2.4.

Table 2.4: Works Related to Energy Efficiency in uplink perspective in a UAV-assisted communication System

Work	**Objective**	**Constraints**	**Methodology/ Algorithm**
[42]	Maximize the system throughput by jointly optimizing the 3D UAV trajectory, communication scheduling, and UAV access point/sensor node transmit power.	Transmit power and UAV trajectory constraint.	Polyblock outer approximation (POA) and SCA

Continued on next page

Table 2.4 – *Continued from previous page*

Work	**Objective**	**Constraints**	**Methodology/ Algorithm**
[43]	UAV's uplink cell associations and power allocations over multiple resource blocks are jointly optimized to maximize the weighted sum rate.	Maximum transmit power constraint, One resource block can be used only for one link in a given time.	Centralized approach through SCA, Decentralized approach through applying SCA for individual clusters
[44]	Studies the energy tradeoff between the UAV and its served sensor.	Maximum transmit power constraint.	Analytical approach as the path is simplified.
[45]	Maximize the energy efficiency of the system.	Maximum transmit power constraint.	Dinkelbach's algorithm and SCA.

After analyzing the above works, we identified that transmit power plays a significant role in uplink communication in terms of energy efficiency, especially for data collection from sensors. As wireless sensor arrays have minimal energy, the energy consumption for transmission of data via the uplink is a crucial factor to be efficiently handled. Moreover, the existing works do not consider transmit power fairness among the wireless sensor nodes (WSNs).

All things considered, our second work focuses on the problem of UAV deployment in the WSN system, increasing energy efficiency while maintaining transmit power fairness among the nodes. It is thoroughly discussed in chapter 4.

Chapter 3

Intelligent UAV Deployment for a Disaster-Resilient Wireless Network

3.1 Overview

In general, three main UAVs' applications in wireless communications have been recognized: A UAV may be used as an aerial base station (ABS), an aerial relay, or an aerial mobile station (MS). From these applications, deploying UAVs as ABSs to enhance the coverage and capacity of terrestrial wireless systems has attracted significant research attention. Potential applications include supplementing the overloaded terrestrial network due to large crowds and providing temporary coverage in areas where the terrestrial network is unavailable due to a natural disaster or an emergency situation [2, 8]. Here, we propose a scheme to optimally position a set of ABSs to provide network coverage to users who have lost connectivity to the terrestrial base station (BS) due to a disaster situation.

The quick deployment capability, high mobility, and low capital expenditure of UAV ABSs make them effective solutions in the above scenarios [1]. Furthermore, UAV ABSs increase the probability of line of sight (LoS) links, which enhance the received signal quality compared to non-line of sight (NLoS) links available in terrestrial BS networks. However, the successful deployment of UAVs as ABSs demands overcoming several challenges. Complex control mechanisms is essential for higher mobility [1] and effective trajectory planning, while self-organization is required for on-demand deployment [13]. Also, the higher probability of LoS links

increases the co-channel interference (CCI). Hence, the control algorithm plays a vital part in these types of networks, as it should focus on several aspects that ensure the system's proper functioning. These include spectrum management, interference mitigation, channel prediction, deployment, user association, energy efficiency, and trajectory planning. Therefore, significant research attention has been focused on intelligent planning of UAV networks recently.

The recent works on UAV networks mainly focus on network coverage [15, 47, 16, 46, 18], quality of connectivity [48], network topology [49], target tracking [50], and utilizing the UAVs as ABSs to serve the user equipments (UEs). In general, all UAV ABSs are connected to each other and to a central control station [51, 15, 16, 46, 18, 48, 49, 50, 27, 52]. The works in the literature consider both centralized [53, 15, 16, 19, 54, 25, 55] and decentralized approaches [18, 56, 57, 58] for the deployment and control of UAV networks. Centralized algorithms are capable of providing highly accurate decisions compared to the decentralized approaches. However, the requirement of having global information at a central location may lead to significant overhead and delay, depending on the application. In contrast, distributed algorithms share limited information and make intelligent decisions through locally available data, resulting in lower overhead and delay in the system. However, as distributed algorithms completely rely on device intelligence and local information, limitations on device intelligence and inaccurate information may lead to system failure. In our work, we propose two low complexity ABS positioning algorithms and a UE assignment scheme, which deems a centralized approach more feasible.

Energy efficiency is paramount for ABSs as the power supply is restricted. There are several techniques introduced to alleviate this issue such as radio frequency energy harvesting, wireless power transfer [59], simultaneous information and power transfer, and self-interference exploitation [7]. However, it is well known that the energy spent in maneuvering the UAVs dominates the energy efficiency, thus UAV deployment and trajectory optimization are crucial for the success of such a network. There are algorithmic approaches [16] that study the deployment problem, with a focus on increasing the energy efficiency without sacrificing the quality of service (QoS) requirements. To this end, machine learning (ML)-based deployment approaches facilitate comparatively quick responses and lower data overheads. In [17], genetic algorithm (GA) and reinforcement learning are used for optimal deployment and user assignment. Similarly, GA with the hill

climbing algorithm (HCA) is used in [24] to enable the communication services and explore the unidentified victims. In [24], initial deployment is done through GA and then the HCA is used to adapt the system to the conditions.

Apart from machine learning algorithms, heuristic algorithms have also been used to solve the UAV placement problem. Although heuristic approaches do not always guarantee the global optimum, can be useful in many applications. Heuristic approaches find an optimal solution without searching over the entire problem space. Therefore, it outperforms typical exhaustive approaches in terms of number of iterations or latency. However, the computational intensity increases exponentially with the number of dimensions of the problem space in heuristic approaches. One example for a heuristic approach is particle swarm optimization (PSO). This optimization approach is originally proposed by J. Kennedy and R. Eberhart in 1995 [60]. The inspiration of this algorithm is the behavior of a bird flock. The PSO-based 3D placement of ABSs is studied in [61]. Although PSO provides superior average performance, the performance for a given instance cannot be guaranteed as it follows a heuristic approach. Therefore, completely relying on PSO may result in severe performance degradation.

A significant contribution is made in [27] with regards to UAV deployment, and this can be considered to be the most related reference to our work. In [27], the authors have used a matching algorithm and a clustering algorithm to find the best 2D position and the UE assignment for a given altitude. Then, a game theoretic approach is used to find the optimal altitudes of the ABSs. Initially, the ABSs are randomly placed in the area of interest, and the ABSs continuously move in the 2D plane until they reach the best 2D position. Subsequently, the altitudes of the ABSs are changed based on the aforementioned game theoretic approach, and the 2D positions and the UE assignments are further fine tuned taking the adjusted altitudes into consideration. This iterative process continues such that the ABSs repetitively change their locations until they reach the optimal positions. A main drawback of this approach is the time and the energy spent in continuously moving the ABSs. It is important to note that the time spent for UAV maneuvering is significantly large compared to the channel coherence time. Therefore, in a practical scenario, the estimated channel state information (CSI) can be less accurate and cause performance degradation. Furthermore, the energy limitations of ABSs have not been taken into account in [27]. There are several other limitations and assumptions found in the literature that do not fully

reflect realistic attributes of UAV ABSs. For example, in [17], an interference-free environment is assumed and CCI is neglected. However, due to the higher probability of LoS propagation in the ABS to UE links, CCI from other ABSs is inevitable.

Considering the limitations of the previous work, in this section we propose a centralized and less complex approach that relies on the average statistics of the channel and eliminates the necessity to continuously move the ABSs. The only information required at the central controller (CC) is the locations of the UEs and the initial locations of the ABSs. With the available location data, we find the optimal locations of the ABSs and the UE assignment for each ABS at the CC, where there is sufficient computational power to provide a rapid solution. According to the decision of the CC, the ABSs can directly change their position from the initial position to the optimal position in one step, making it a quick and energy efficient approach.

The deployment problem is divided into three phases, which are 2D deployment, UE assignment, and the altitude selection. The approach taken for 2D deployment and the UE assignment has similarities to [27] as they stem on a clustering algorithm and a matching algorithm, respectively. The approaches significantly differ in the third step, which is the altitude selection. We propose two methods for altitude selection. The first method performs an exhaustive search among a discrete set of altitude values, without allowing altitude diversity among ABSs. This means all ABSs operate at a common altitude. We effectively truncate the search space by using properties of our objective function. On the other hand, the second method facilitates altitude diversity, and the altitudes of the ABSs are decided through a PSO algorithm. Our proposed algorithms keep track of the available energy in the batteries of the ABSs, and take them into consideration in making the decision on the ABS deployment, making them further different from the schemes proposed in [27].

Our work considers the impact of CCI in the ABS deployment process. Furthermore,we focus on fully utilizing the spatial diversity by deploying omnidirectional antennas. In addition, being different to our work, the impact of LoS is not considered in [7, 47, 17, 62] for small-scale fading, which can significantly affect the performance in dense urban environments. Moreover, the altitude of the UAVs are not taken into account in [24, 25], and a fixed UAV altitude assumption is considered in [15]. It is well known that the altitude of the UAV plays a

major role in the performance of the network, due to its impact on the path loss, coverage radius, and the probability of line of sight (PLoS). In our work, we have considered a feasible altitude range to exploit the gain from altitude diversity.

The novelty and the key contributions of the work that is proposed in this section can be summarized as follows.

- A multi-UAV and multi-UE system, where UEs are randomly distributed in a disaster struck area is considered.
- Algorithms are proposed to position the UAV ABSs and allocate UEs for each ABS, to maximize the sum spectral efficiency of the network, while maintaining a minimum QoS level for all UEs.
- The proposed scheme is centralized and has a low level of complexity, as only the statistical CSI, locations of the UEs, and the initialized locations of the ABSs are required as inputs.
- The proposed scheme allows the ABSs to directly move from their initial position to the optimal position with a single maneuver, making it a quick and energy efficient approach.
- The available energy levels in the batteries of the ABSs are taken into consideration in the deployment.

The remainder of this chapter is organized as follows. In Section 3.2, we present our system model. Section 3.3 describes the proposed ABS placement and UE association schemes. Section 3.4 presents numerical results and insights, while Section 3.5 concludes this chapter.

3.2 System Model

3.2.1 Spatial Model

Consider an area $\mathbb{A}$ where the UEs are distributed following a homogeneous Poisson point process (PPP) with intensity of λ_U in the 2-dimensional Euclidean space $\mathbb{R}^2$. Due to a disaster, the UEs located inside the circular region of radius R_B denoted by $\mathbb{B}$ (centered at the origin of $\mathbb{A}$) have lost connectivity with the terrestrial network. Figure 3.1 illustrates a sample UE distribution. Hereafter, we only focus on the UEs in region $\mathbb{B}$. The average number of UEs in $\mathbb{B}$ is N_{UE}.

To serve these UEs, N_{UAV} UAVs are deployed as ABSs. It is assumed that the maximum number of UEs supported by an ABS is N_T. Therefore, on the average, we have

$$N_{\text{UAV}} = \left\lceil \frac{N_{\text{UE}}}{N_T} \right\rceil , \tag{3.1}$$

where the operator $\lceil . \rceil$ represents the ceiling function.

Initially, the ABSs are deployed randomly in the 3-dimensional space above $\mathbb{B}$. Let S_j denote the coordinates of the jth ABS. S_j takes the form of (x_j, y_j, H_j), where x_j and y_j represent the location of the jth ABS in $\mathbb{R}^2$ and H_j represents the altitude of the jth ABS. We define $\mathcal{S} = \{S_1, \ldots, S_{N_{\text{UAV}}}\}$. B_i represents the location of the ith UE. Let ϕ_j denote the set of UEs associated with the jth ABS. We define the set $\Phi = \{\phi_1, \ldots, \phi_{N_{\text{UAV}}}\}$, such that the sum of the cardinalities of ϕ_j, $j \in \{1, 2, \ldots, N_{\text{UAV}}\}$ is N_{UE}, i.e., $\sum_j |\phi_j| = N_{\text{UE}}$. Moreover we assume that a UE cannot communicate with more than one ABS, thus the elements in Φ are disjoint, i.e., $\phi_j \cap \phi_i = \emptyset$ for $\forall i \neq j \in \{1, \ldots, N_{\text{UAV}}\}$.

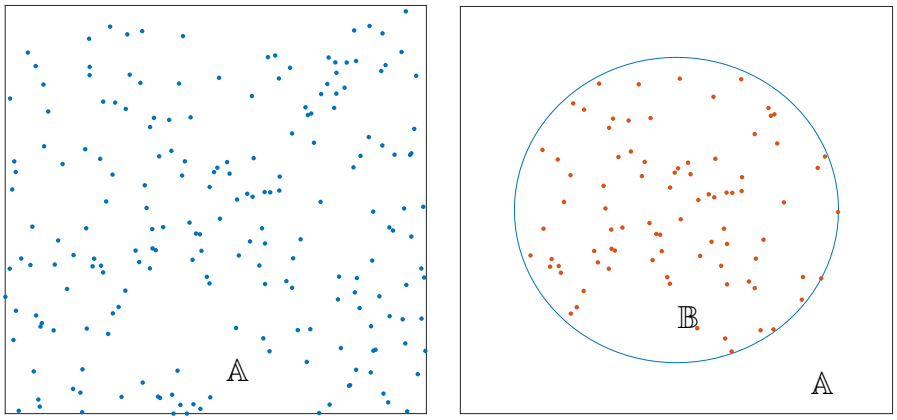

Fig. 3.1: (**a**) User equipment (UE) distribution in $\mathbb{A}$ and (**b**) UE distribution in $\mathbb{B}$ (disaster region).

The ABSs have limited battery resources, and it is assumed that they cannot be recharged while in operation. For simplicity, we consider equal initial battery life at all ABSs. The available energy in batteries is used for both ABS maneuvering and data transmission. The total energy available for maneuvering is denoted by E_T. Although having equal battery power at initialization, the battery levels among ABSs shall differ while in operation, as per the distance traveled. Thus, each ABS keeps track of the available energy in the battery. The energy remaining for the maneuvering of the jth ABS is denoted by E_j. Considering a single

maneuver of the jth ABS, the energy required to move the ABS from the present location (a_j^0, b_j^0, c_j^0) to the new location (a_j, b_j, c_j) is estimated using

$$E_{\text{mob}}^j = \eta_h[(a_j^0 - a_j)^2 + (b_j^0 - b_j)^2]^{1/2} + \eta_v[c_j^0 - c_j)^2]^{1/2}, \tag{3.2}$$

where η_h and η_v denote the energy consumption for movement per unit distance in the horizontal and vertical directions, respectively.

3.2.2 Channel Model

As UEs are only served by ABSs, we only focus on the ABS-UE channel. This channel experiences both LoS and NLoS propagation conditions depending on the altitude of the ABSs. Therefore, it is essential to consider both LoS and NLoS links in a realistic performance evaluation. The probability of communicating through a LoS ABS-UE link can be calculated based on the elevation angle of an ABS with respect to a UE using the following originally given in [14],

$$P(LOS, \theta_j^i) = \frac{1}{1 + a\exp(-b[\theta_j^i - a])} \ , \tag{3.3}$$

where θ_j^i is the elevation angle of the jth ABS with respect to the ith UE, and a and b are environment dependent parameters.

By considering the effects of LoS and NLoS propagation, the channel gain from the jth ABS to the ith UE is modeled as

$$h_q(j,i) = \frac{|g_q|^2}{\sqrt{(H_j^2 + d(j,i)^2)^{\alpha_q}}} \ , \tag{3.4}$$

where $q \in \{L, N\}$ such that L and N refer to the LoS and NLoS conditions, respectively, g_q is the small-scale fading amplitude, $d(j,i)$ is the distance between the jth ABS and the ith UE, α_q is the large-scale path loss exponent [63], and we assume $\alpha_L < \alpha_N$. It is also assumed that g_L follows a Rician fading distribution with the Rice factor K, while g_N follows the Rayleigh fading distribution.

3.2.3 Signal-to-Interference-plus-Noise Ratio (SINR)

Considering the interference from other co-channel ABSs is crucial when positioning an ABS[8]. In contrast to the works in [8, 47, 17], we consider the full

impact of CCI in the ABS placement and UE association problems. Figure 3.2 illustrates a sample scenario of our proposed system. The SINR of the ith UE associated with the jth ABS is given by

$$SINR(j,i) = \frac{P_r(j,i)}{I_{\text{Agg}}(i) + N_0} \ , \tag{3.5}$$

where $P_r(j,i)$ is the signal power received at the ith UE from the jth ABS, $I_{\text{Agg}}(i)$ is the aggregate interference experienced by the ith UE, and N_0 is the power spectral density of the Gaussian noise. In addition, the received signal power $P_r(j,i)$ can be expressed as

$$P_r(j,i) = p_t^j[P(LOS,\theta_j^i)h_L(j,i) + (1 - P(LOS,\theta_j^i))h_N(j,i)] \ , \tag{3.6}$$

where p_t^j is the transmit power of the jth ABS. The aggregate CCI is given by

$$I_{\text{Agg}}(i) = \sum_{l=1,l\neq j}^{N_{\text{UAV}}} p_t^l[P(LOS,\theta_j^i)h_L(j,i) + (1 - P(LOS,\theta_j^i))h_N(j,i)], \tag{3.7}$$

where we have incorporated the effect of both LoS and NLoS propagation from the interfering ABSs.

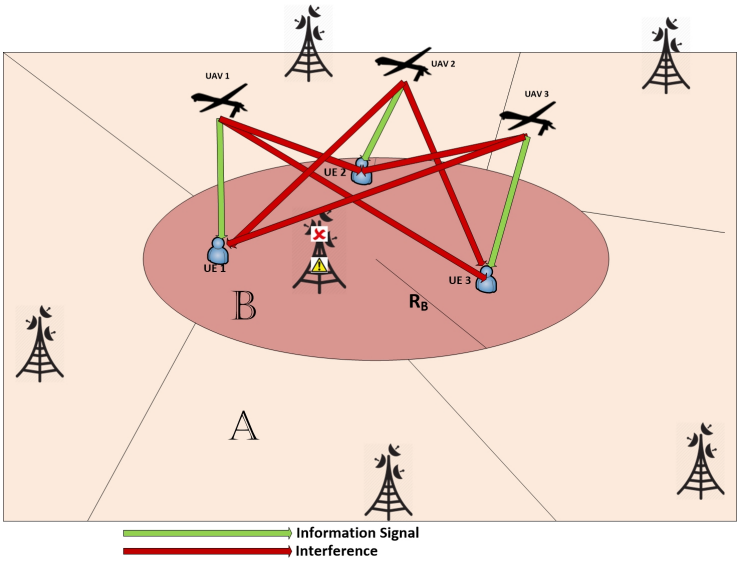

Fig. 3.2: System model illustration of the information and interference signals for $N_{\text{UAV}} = 3$ and $N_{\text{UE}} = 3$.

3.3 Optimal ABS Placement and User Association

In this section, we focus on inferring $\mathcal{S}$, the position of each ABS, and Φ, the assigned UE list for each ABS such that the total spectral efficiency (TSE) of the network is maximized. The TSE is given by

$$TSE = \sum_{j=1}^{N_{\text{UAV}}} \sum_{i \in \phi_j} \log_2 \left[1 + SINR(j,i)\right]. \tag{3.8}$$

The optimization problem of interest can be formulated as follows:

$$\begin{aligned} \max_{\mathcal{S},\Phi} \quad & TSE \\ \text{s.t.} \quad & E^j_{\text{mob}} \leq E_j, \\ & SINR(j,i) \geq SINR_{\min}, \quad i \in \phi_j,\ j \in \{1,\ldots,N_{\text{UAV}}\}, \\ & \sum_{j=1}^{N_{\text{UAV}}} |\phi_j| = N_{\text{UE}}, \\ & \phi_j \cap \phi_i = \emptyset, \quad \forall i \neq j \in \{1,\ldots,N_{\text{UAV}}\}, \\ & |\phi_j| \leq N_T \quad j \in \{1,\ldots,N_{\text{UAV}}\}, \end{aligned} \tag{3.9}$$

where $SINR_{\min}$ is the SINR threshold set to ensure the minimum QoS requirement.

It is clear that the objective function and the constraints of (3.9) are non-convex and it is challenging to obtain an optimal solution with polynomial complexity. A problem very similar to (3.9) has been solved in [27] using game theory combined with an iterative algorithm. Figure 3.3 illustrates an example ABS placement and UE association obtained using the approach in [27]. To reach this solution, in [27], it has been assumed that the small-scale fading process is stationary and the UEs and the ABSs have full knowledge of the CSI. However, it is important to note that the time it takes to move an ABS can be significantly larger than the coherence time of the channel, leading to decisions based on outdated CSI. Furthermore, it is important to note that the ABSs have to execute multiple maneuvers to reach the optimal 2D position, resulting in high energy consumption. Therefore, we consider a novel approach where only the statistical CSI and the locations of the UEs and the ABSs are used to determine

the optimal 2D position and the UE assignment. In addition, we use a centralized approach to solve the placement and UE association problem, and move the ABSs to their optimal positions using a single maneuver to reduce the overall energy consumption.

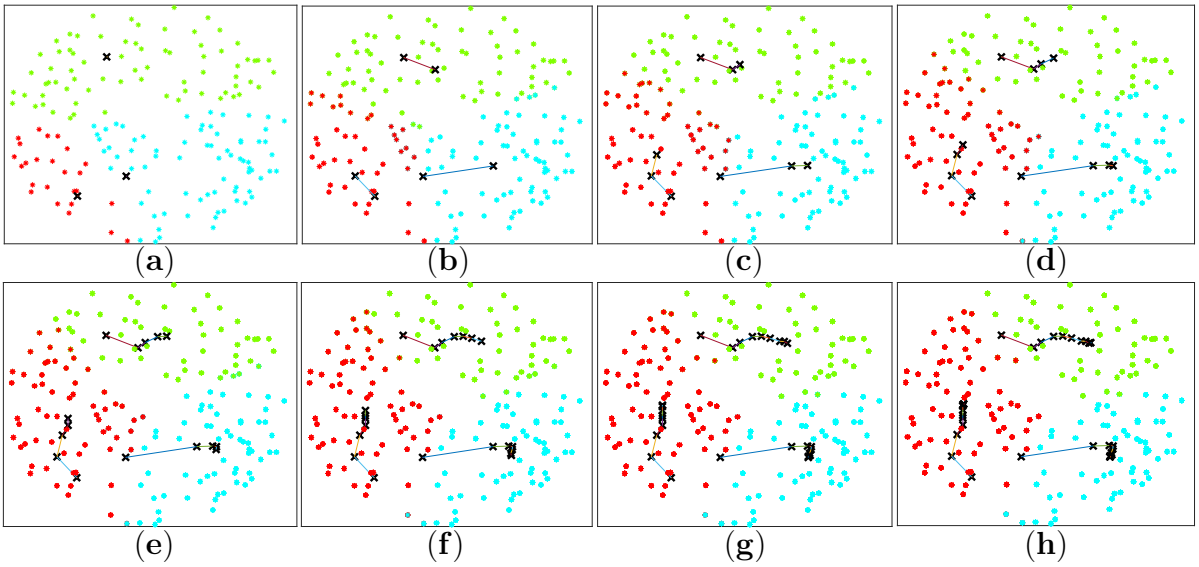

Fig. 3.3: Illustration of ABS placement and UE association obtained using the approach in [27], where $R_B = 2000$ m, $\alpha_N = 2.5$, $\alpha_L = 2$, $\lambda_U = 2 \times 10^{-4}/\text{m}^2$, $\delta = 0$, $N_{\text{UAV}} = 3$, H^*= 300 m, $N_T = 70$. The position of the ABS is represented using $\mathbf{X}$. The three colors differentiate the UE clusters at a particular stage. (**a**–**h**) illustrate the 1st,...,5th, 7th, 9th and 11th adaptive stages, respectively

To this end, this work defines a new SINR parameter based on statistical CSI and we refer to it as the *statistical SINR* (SSINR). The SSINR of the ith UE associated with the jth ABS is given by

$$SSINR(j,i) = \frac{\mathbb{E}[P_r(j,i)]}{\mathbb{E}[I_{\text{Agg}}(i)] + N_0} \ , \tag{3.10}$$

where $\mathbb{E}[\cdot]$ denotes the expectation. From (3.4), (3.6), and (3.7), it can be identified that $SSINR(j,i)$ can be computed using the knowledge of UE and ABS positions and the statistics of Rayleigh and Rician fading. Therefore, compared to instantaneous CSI, a significantly lower overhead is required to make these information available at the CC. Using SSINR, we reformulate the optimization problem as

$$\begin{aligned} \max_{\mathcal{S},\Phi} \quad & STSE \\ \text{s.t.} \quad & SSINR(j,i) \geq SINR_{\min}, \quad i \in \phi_j,\ j \in \{1,\ldots,N_{\text{UAV}}\}, \end{aligned} \tag{3.11}$$

where the constraints not shown remain unchanged from (3.9), and $STSE$ is defined as

$$STSE = \sum_{j=1}^{N_{\text{UAV}}} \sum_{i \in \phi_j} \log_2 \left[1 + SSINR(j,i)\right], \tag{3.12}$$

which can be interpreted as the achievable TSE when $SINR(j,i)$ is approximated by $SSINR(j,i)$, and we refer to STSE as *statistical total spectral efficiency*. It is not hard to recognize that (3.11) is also non-convex and cannot be solved using algorithms with polynomial complexity. Therefore, we propose to solve (3.11) using a 3-step approach, namely, the 2D deployment of the ABSs, UE assignment, and altitude selection of the ABSs. This chapter first presents a methodology for the 2D deployment of the ABSs and the UE assignment.

3.3.1 2D Deployment of the ABSs and the UE Assignment

Initially, all ABSs are randomly and uniformly placed above the disaster zone. The ABSs then estimate the locations of the UEs in its region of coverage from the uplink signals. These locations are sent to a centralized location, together with the locations of the ABSs, such that the centralized location is fully aware of the network topology. Using this knowledge, the user assignment and the 2D positioning follows an iterative three step process. Note that all of these iterations take place at the centralized location. First, the received SSINR values at each UE from the ABSs providing coverage are calculated. Second, using the calculated SSINRs, the UE assignment to the ABSs is performed through a stable marriage approach. The goal is to assign the UEs to the ABS providing the best SSINR such that the constraint on the maximum UEs per ABS is not violated. Therefore, in the stable marriage approach, the UE assignment is done such that both these parties (UEs and ABSs) are jointly satisfied with a particular assignment, and there is no other UE assignment that the two parties would rather prefer having than the current assignment. If there are no such other assignments, the matches are deemed stable. Once each UE is assigned to an ABS, the third step of the 2D deployment of the ABSs is done through a clustering algorithm. The clustering algorithm proposed in this chapter closely follows the principles of K-means clustering. However, in contrast to conventional K-means clustering, our algorithm uses multiple weighting parameters in the decision phase. Essen-

tially, the locations of the ABSs are updated such that they coincide with the centroid of the locations of their assigned UEs in the 2-dimensional Euclidean space, denoted by $(x_c, y_c, 0)$. This three step process continues until the exit condition is satisfied. The statistical total spectral efficiency gain denoted by G_{L} is used as the metric to determine the algorithm convergence. To this end,

$$G_{\mathrm{L}} = \psi^n - \psi^{n-1}\,, \tag{3.13}$$

where ψ^n is the STSE in the nth iteration. The iterative process continues as long as G_{L} is greater than δ, which is the least expected gain from an iteration. Note that the physical locations of the ABSs do not change iteratively, thus they can hover at the initialized location until a decision is made on the optimal location. Figure 3.5 illustrates the movement of the ABSs in the 2D plane after finding the best 2D position through CC.

3.3.2 ABS Altitude Selection

We present two approaches for the altitude selection. In the first approach, the altitude diversity is not considered and all ABSs are assumed to be at the same optimal altitude, denoted by H^*. Once the initial optimal 2D positions are determined, an exhaustive search over a discrete set of altitudes is used to find the optimal altitude for the ABSs. For each altitude, the 2D locations and UE assignments are further fine-tuned, using the same three-step iterative process described earlier. To limit the search space in the exhaustive search, we make the following observations regarding the received SSINR of a UE. Considering the impact of the ABS altitude in the downlink, it is shown in [14] that when CCI is not present, the received signal power increases in the beginning and decreases after a certain point, indicating the existence of an optimal altitude where the received power is maximum. This behavior can be explained using the combined effect of path loss and the probability of line of sight. The path loss increases with the ABS altitude, resulting in the degradation of the signal quality. However, increasing the altitude also leads to higher $P(LOS, \theta)$, which in turn results in better signal quality. Once the altitude increases beyond a critical point, the improvement in $P(LOS, \theta)$ becomes negligible compared to the signal power degradation due to path loss. Therefore, the received signal power increases in the beginning and decreases after a certain point, when the altitude of

the ABSs hovering at ground level is increased. However, the reasoning is slightly different when CCI is considered. For a typical UE, the interfering ABSs have larger link lengths compared to the connected ABS, when the ABSs are at lower altitudes. Therefore, the interference power is smaller compared to the desired signal power at lower altitudes. Thus, the SSINR will behave similarly to the case with no CCI. In higher altitudes, the SSINR degrades due to two factors. First, the path loss increases and starts to dominate the desired signal power compared to the effect from $P(LOS, \theta)$. Second, the increased elevation angles with the interfering ABSs further increase the interference power. Therefore, the SSINR decreases continuously after a critical altitude. This means the STSE increases with the common altitude of the ABSs up to a certain altitude level, and then decreases monotonically. This intuition is used to limit the search space of the exhaustive search, as there is no advantage searching if the objective function is in the decreasing trend. Therefore, in the first approach, the common ABS altitude is increased until the STSE begins to decrease, and an optimal altitude is found accordingly. These ideas are formally stated in Algorithm 1. Notations used in the algorithms are tabulated in Table 3.1.

The second approach, which we present as Algorithm 2, resorts to the same approach for 2D positioning of the ABSs and for user association as in Algorithm 1. However, Algorithm 2 uses particle swarm optimization (PSO) to set the altitude values of the ABSs. The approach facilitates altitude diversity. PSO is an intelligent algorithm that stems on the approach used by a group of birds for searching food or for traveling long distances. Essentially, this algorithm keeps track on two positions, namely the local best (LB) and the global best (GB). $W_k^{\mathrm{Lb}}(n)$ denotes the LB of the kth particle in the nth iteration, and $W^{\mathrm{Gb}}(n)$ is the GB in the nth iteration. The LB gives us the optimal solution (position) for a particular particle where as the GB gives us the optimal solution (position) among all the particles. The velocity vector of a particle is calculated based on the LB, the GB and the inertia of the particle. To this end, the velocity of the kth particle during the nth iteration is given by

$$V_k(n) = \xi V_k(n-1) + c_1\varphi_1(W_k^{\mathrm{Lb}}(n-1) - W_k(n-1)) + c_2\varphi_2(W_k^{\mathrm{Gb}}(n-1) - W_k(n-1)), \tag{3.14}$$

where ξ is the inertia weight that controls the exploration ability, φ_1 and φ_2 are positive random numbers, and c_1 and c_2 denote the local learning coefficient and the swarm learning coefficient, respectively. Moreover, the position of the kth

particle in the nth iteration is updated according to

$$W_k(n) = W_k(n-1) + V_k(n). \tag{3.15}$$

The movement of the kth particle in the PSO problem space is illustrated in Figure 3.4. The next position of each particle in the PSO space will be decided upon three vectors, which are the GB vector, the LB vector, and the previous velocity vector.

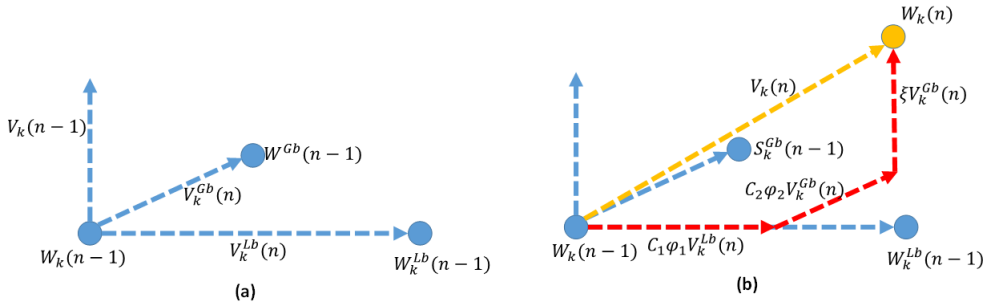

Fig. 3.4: (**a**) Global best, local best, position, and the velocity in the $(n-1)$th iteration. (**b**) Velocity in the nth iteration as a weighted vector addition of previous velocity components and the position in the nth iteration.

With regards to our problem, Algorithm 2 initializes the PSO population with their positions. Each particle is a vector of size of N_{UAV}, such that its jth element represents the altitude of the jth ABS. Initially, the altitude values in all particles, i.e., each element in the vector, are set randomly and uniformly between the minimum and the maximum allowable altitudes. These values are used to initialize the LB of each particle, and the initial velocity of each particle is set to one. For each particle, i.e., for each altitude vector, the corresponding optimal UE assignment and the optimal 2D position allocation are obtained through **Block-A** of Algorithm 1. Then, the objective function, which is the STSE, is evaluated for each particle considering the current UE and the position assignments. Their initial position is the LB for all the particles and is also based on these calculated values; the GB position vector of the swarm will be updated. This ends the initialization stage.

Then, the iterative process of finding the best set of locations begins. The velocity and the altitude of each particle are updated as per (3.14) and (3.15), respectively. For each particle, i.e., for each altitude vector, the corresponding optimal UE assignment and the optimal 2D position allocation are obtained through

Algorithm 1: Clustering and matching algorithm with exhaustive search.

Data: S_j, B_i $\quad i \in \{1,\ldots,N_{\mathrm{UE}}\}$ and $j \in \{1,\ldots,N_{\mathrm{UAV}}\}$
$h_l \Leftarrow$ common altitude of the ABS. $\quad l \in \{1,\ldots,N_H\}$
Result: $\mathcal{S}^*$ and Φ^*
begin
for $l = 1,\ldots,N_H$ **do**
Block-A
$n = 1 \Leftarrow$ Iteration index
$\psi^0 = 0$
while $n \geq 0$ **do**
for $j = 1,\ldots,N_{UAV}$ ***and*** $i = 1,\ldots,N_{UE}$ **do**
SSINR calculation
$SSINR(j,i) = \frac{\mathbb{E}[P_r(j,i)]}{\mathbb{E}[I_{\mathrm{Agg}}(j)]+N_0}$
User Assignment
$\mathcal{L}_i^{\mathrm{UE}} \Leftarrow$ Ordered preference vector of the ith UE
$\mathcal{L}_j^{\mathrm{UAV}} \Leftarrow$ Ordered preference vector of the jth ABS
$N_j^C \Leftarrow$ Number of UEs connected to jth ABS
for $k = 1,\ldots,N_{UAV}$ **do**
for $i = 1,\ldots,N_{UE}$ **do**
for $j = 1,\ldots,N_{UAV}$ **do**
$e = \mathcal{L}_j^{\mathrm{UAV}}(i) \Leftarrow i$th UE preference of $j^{\mathrm{th}}ABS$
if $\mathcal{L}_e^{UE}(k) = j)$ ***and*** $N_j^C \leq N_T$ **then**
$i \in \phi_j$
$N_j^C = N_j^C + 1$
$\Phi^* = \{\phi_j\}_{j=1}^{N_{\mathrm{UAV}}}$
$\psi^n = \sum_{j=1}^{N_{\mathrm{UAV}}} \sum_{i\in\phi_j} \log_2\left[1 + SSINR(j,i)\right]$
$G_{\mathrm{L}} = \psi^n - \psi^{\mathrm{n\text{-}1}}$
if $G_L \leq \delta$ **then**
break
for $j = 1,\ldots,N_{UAV}$ **do**
2D Postioning
$(x_j, y_j) = D_j \Leftarrow$ centroid of the 2D locations of the UEs in ϕ_j
Calculate the energy needed for the maneuvering E_{mob}^j as per (3.2)
if $E_j \leq E_{mob}^j$ **then**
break
$n = n + 1$
$STSE\,(l) = \sum_{j=1}^{N_{\mathrm{UAV}}} \sum_{i\in\phi_j} \log_2\left[1 + SSINR(j,i)\right]$
if $STSE\,(l) \leq STSE\,(l-1)$ **then**
break
Calculate the energy needed for the maneuvering E_{mob}^j as per (3.2)
if $E_j \leq E_{mob}^j$ **then**
break
$H^* = h_k \mid k = \arg\max_l STSE(l)$
$\mathcal{S}^* = \{(x_j, y_j, H^*)\}_{j=1}^{N_{\mathrm{UAV}}}$

Table 3.1: Table of notations.

Notation	Description
x_j, y_j	2D- Coordinates of the jth ABS
B_i	2D- Coordinates of the ith UE
λ_U	Intensity of the UE distribution
R_B	Radius of the isolated region
N_{UAV}	Required Number of UAVs
N_{UE}	Number of UEs in the isolated region
N_T	Maximum number of UE that can be supported by an ABS
$d(j,i)$	2D euclidean distance from jth ABS to ith UE
α_q	Large-scale path loss exponent
g_q	Small-scale fading amplitude
p_t^j	Transmission power of the jth ABS
$P_r(j,i)$	Received signal power at ith UE from the jth ABS
$I_{\text{Agg}}(i)$	Aggregated interference experienced by the ith UE
E_{mob}^j	Required energy for mobility of the jth ABS
E_j	Available energy for mobility at the jth ABS
η_h , η_v	Energy consumption per unit distance to horizontal and vertical movement respectively
ϕ_j	Assigned user list of the jth ABS
$P(LOS, \theta_j^i)$	probability of line of sight from jth ABS to the ith UE
a , b	Constants which reflects environmental characteristics
$h_q(j,i)$	Channel gain from the jth ABS to the ith UE
$SINR_{\min}$	Minimum SINR threshold which reflects the minimum QoS requirement
G_L	Gain achieved comparing to the previous step
H_j	Altitude of the jth ABS
H^*	Common optimal altitude
N_H	Number of discrete altitude levels considered in Algorithm 1
H_j^*	Optimal altitude of the jth ABS
δ, $\tilde{\delta}$	Minimum gain expected in Algorithm 1 and Algorithm 2
$h_{\min}$,$h_{\max}$	Minimum and maximum altitude allowed to hover an ABS
$W_k(n)$	Position of the k^{th} particle at nth iteration in PSO space
$W^{\text{Gb}}(n)$	Global best position at the nth iteration in PSO space
$W_k^{\text{Lb}}(n)$	Local best position of the k^{th} particle at nth iteration in PSO space
$V_k(n)$	Velocity of kth particle at nth iteration in PSO space
$J_k(n)$	Objective function value of the kth particle at nth iteration in PSO space
c_1, c_2	Local learning coefficient and swarm learning coefficient respectively
ξ	Inertia weight of the swarm particle
N_{pop}	Number of particles in the swarm population
G_P	Spectral efficiency gain achieved comparing to the previous iteration in PSO
N_G	Number of continuous iterations without a gain in the spectral efficiency
Γ	Threshold to exit the PSO algorithm

Block-A of Algorithm 1. The objective function is computed again for the newly updated positions, and the LB and GB positions are updated consequently.

The iterative process continues until the STSE gain between two subsequent iterations, denoted by G_P, is below a certain predefined threshold. More precisely, if there are Γ subsequent iterations where the G_P is less than a predetermined threshold value $\tilde{\delta}$, the iterative process stops and the PSO is assumed to have reached convergence. At convergence, GB contains the altitude vector for the ABSs that maximizes the TSE as per Algorithm 2. These ideas are formally stated in Algorithm 2.

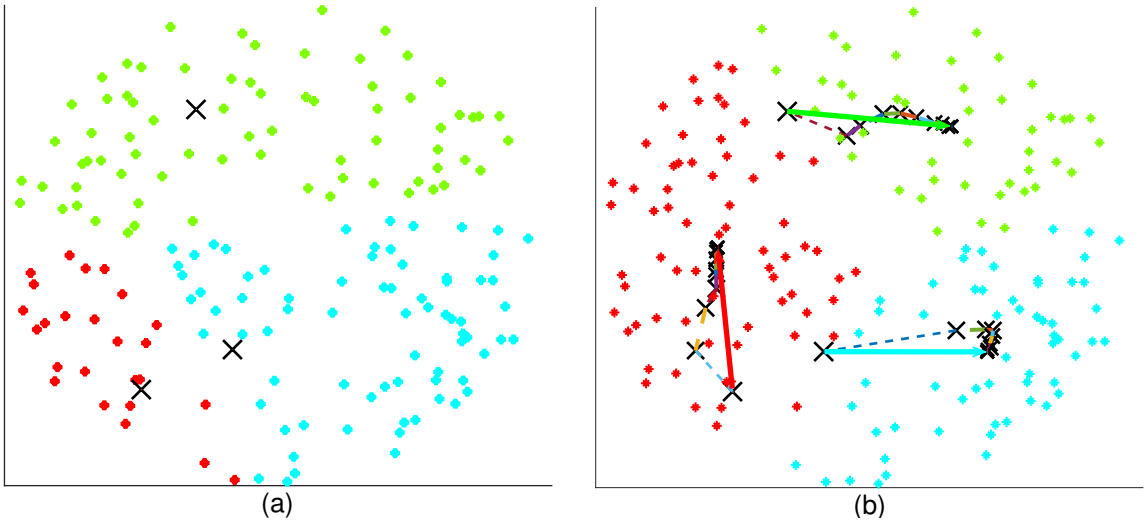

Fig. 3.5: Illustration of the movement of the aerial base stations (ABSs) in the 2D plane for suburban environment. The position of the ABS is represented using $\mathbf{x}$. The three colors differentiate the UE clusters of the respective ABSs. (**a**) Initial 2D position of the ABSS. (**b**) Movement of the ABSs to the computed position. The solid arrow represents the actual ABS movement. The doted lines represent the adaptive process (does not represent the movement) performed at the CC. $R_B = 2000$ m, $\alpha_N = 2.5$, $\alpha_L = 2$, $\lambda_U = 2 \times 10^{-4}/\text{m}^2$, $\delta = 0$, $N_{\text{UAV}} = 3$, $H^* = 300$ m, $N_T = 70$.

3.4 Simulation Results and Discussion

In this section, the performance of the proposed algorithms is evaluated through extensive simulation results. The results are averaged through 50 000 iteration. The parameters used in the simulations are given in Table 3.2. The algorithms are compared in terms of TSE, energy consumption, and the average coverage

Algorithm 2: Clustering and matching algorithm with PSO

Data: S_j, B_i $\quad i \in\{1,\ldots,N_{\mathrm{UE}}\}$ and $j \in\{1,\ldots,N_{\mathrm{UAV}}\}$
Result: $\mathcal{S}^*$ and Φ^*
begin
  $n = 1 \Leftarrow$ Iteration index
  Initialization
    for $k = 1, \ldots, N_{pop}$ **do**
      $W_k(n) = \{H_1, \ldots, H_{N_{\mathrm{UAV}}}\} \mid H_j \sim \mathcal{U}(h_{\min}, h_{\max})$,
       $j \in\{1,\ldots,N_{\mathrm{UAV}}\}$
      $V_k(n) = 1$
      $W_k^{\mathrm{Lb}}(n) = W_k(n)$
      Run **Block-A** Algorithm 1 with $W_k(n)$ as an input
      Get Φ^* and (x_j, y_j) for $j \in \{1, \ldots, N_{\mathrm{UAV}}\}$
      $J_k(n) = \sum_{j=1}^{N_{\mathrm{UAV}}} \sum_{i\in\phi_j} \log_2 [1 + SSINR(j, i)]$
    $W^{\mathrm{Gb}}(n) = W_r(n) \mid r = \arg\max_k J_k(n)$
  while $N_G < \Gamma$ **do**
    for $k = 1, \ldots, N_{pop}$ **do**
      $V_k(n+1) =$
       $\xi V_k(n) + c_1\varphi_1(W_k^{\mathrm{Lb}}(n) - W_k(n)) + c_2\varphi_2(W_k^{\mathrm{Gb}}(n) - W_k(n))$
      $W_k(n+1) = W_k(n) + V_k(n+1)$
      Run **Block-A** Algorithm 1 with $W_k(n)$ as an input
      Update Φ^* and (x_j, y_j) for $j \in \{1, \ldots, N_{\mathrm{UAV}}\}$
      ;
      $J_k(n+1) = \sum_{j=1}^{N_{\mathrm{UAV}}} \sum_{i\in\phi_j} \log_2 [1 + SSINR(j, i)]$
      if $J_k(n+1) > J_k(n)$ **then**
        $W_k^{\mathrm{Lb}}(n+1) = W_k(n+1)$
      else
        $W_k^{\mathrm{Lb}}(n+1) = W_k^{\mathrm{Lb}}(n)$
    $W^{\mathrm{Gb}}(n+1) = W_r^{\mathrm{Lb}}(n+1) \mid r = \arg\max_k J_k(n+1)$
    Calculate the energy needed (E^j_{mob}) to move the ABSs from
     $W^{\mathrm{Gb}}(n)$ to $W^{\mathrm{Gb}}(n+1)$ as per (3.2)
    if $E_j \leq E^j_{mob}$ **then**
      break
    $G_P = J_r(n+1)$ - $J_q(n) \mid r = \arg\max_k J_k(n+1)$,
     $q = \arg\max_k J_k(n)$
    if $G_P \leq \tilde{\delta}$ **then**
      $N_G = N_G + 1$
    else
      $N_G = 0$
    $n = n + 1$
  $\{H_1^*, \ldots, H_{N_{\mathrm{UAV}}}^*\} = W^{\mathrm{Gb}}(n+1)$
  $\mathcal{S}^* = \{(x_j, y_j, H_j^*)\}_{j=1}^{N_{\mathrm{UAV}}}$

probability, which is computed as

$$\overline{P_{\mathrm{COV}}} = \frac{N_{\gamma_{\mathrm{th}}}}{N_{\mathrm{UE}}} \ , \tag{3.16}$$

where $N_{\gamma_{\mathrm{th}}}$ is the number of users experiencing SINR greater than a threshold value $SINR_{\mathrm{min}}$. In simulations, we consider $\mathbb{A}$ to be a 6×6 km^2 square. To be compatible with the literature, other parameters are set as in Table 3.2. Moreover, the gain thresholds, δ and $\tilde{\delta}$, are set to 0 as we assume static UEs.

Table 3.2: Simulation settings

Parameter	**Value**	**Parameter**	**Value**
λ_u	$4 \times 10^{-4}/\mathrm{m}^2$	R_B	2000 m
N_T	40	E_T	1 kJ
α_L	2	α_N	2.5
p_t^j	30 dBm	δ,$\tilde{\delta}$	0
Γ	4	N_0	-80 dBm
r	15 Mbps	η_h	0.1 J/m
η_v	1 J/m	N_{pop}	20
φ_1, φ_2	random [0,1]	$SINR_{\mathrm{min}}$	-30 dB
h_{min}	50 m	h_{max}	3000 m
ξ	0.5175		
a	4.8800 (Suburban)	b	0.4290 (Suburban)
	9.6117 (Urban)		0.1581 (Urban)
	12.0810 (Dense urban)		0.1140 (Dense urban)
	24.5960 (High-rise urban)		0.1248 (High-rise urban)

Figures 3.6 and 3.7 compare the achievable TSE of Algorithm 1 for different ABS altitudes, with naive random ABS deployment and the equidistant deployment. In naive random deployment, the 2D locations of the ABSs above $\mathbb{B}$ are chosen randomly. The UEs are assigned to the nearest ABS such that each UE is assigned to only one ABS, in a manner that all UEs meet the minimum QoS requirement ($SINR_{\mathrm{min}}$). In equidistant deployment, the ABSs are placed along radial lines that equally partition a circle above $\mathbb{B}$. The ABSs move outwards or inwards radially, until all the UEs meet the minimum QoS requirement $SINR_{\mathrm{min}}$. It can be observed that Algorithm 1 outperforms the random and equidistant de-

ployments. Furthermore, one can note that even though we have used SSINR and STSE in obtaining the solution, the optimal altitude obtained by our algorithm is actually the altitude which provides the maximum TSE for the considered propagation environments.

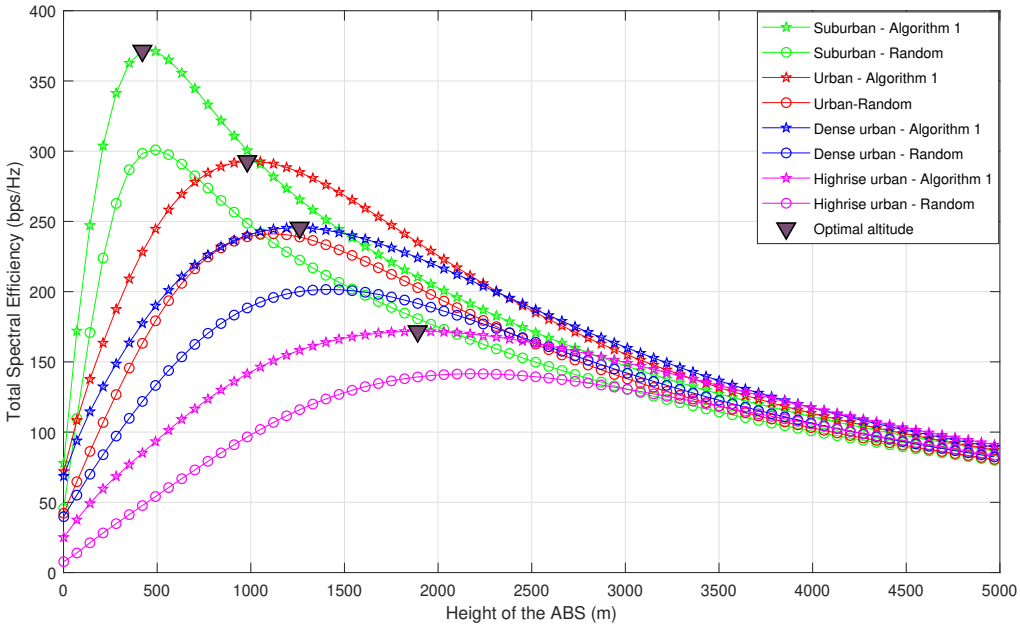

Fig. 3.6: Total spectral efficiency vs. altitude of the ABS (comparison between Algorithm 1-based deployment and random deployment).

Moreover, the optimal altitudes for the considered propagation environments in the ascending order are suburban, urban, dense urban, and high-rise urban. As explained in Section 3.3, the impact of $P(LOS, \theta)$ on the signal quality is dominant until it starts to saturate. It is important to note that the elevation angles at which $P(LOS, \theta)$ begins to saturate also follow the same order. Therefore, the optimal altitude is smallest for suburban environments while it is largest for high-rise urban environments. This is a valuable insight when designing ABSs for different environments, as ABSs must be designed with sufficient energy to reach the optimal altitude. Furthermore, it can be observed that TSE in all scenarios converge to the same value for higher ABS altitudes regardless of the propagation environment. This is because for higher altitudes, regardless of the propagation environment, θ approaches 90°, leading to $P(LOS, \theta) \approx 1$. Therefore, TSE solely depends on path loss, which is almost the same in all environments.

To compare Algorithm 1 with naive random deployment in terms of coverage probability, we evaluate the average coverage probability for each propagation environment, when the ABSs are placed at their optimal altitudes. From Figure

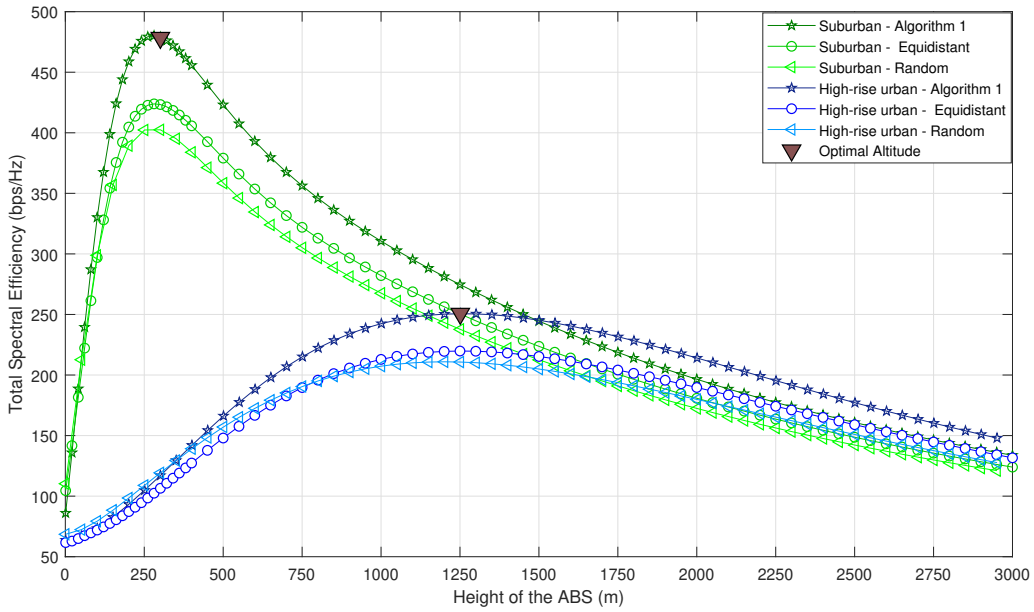

Fig. 3.7: Total spectral efficiency vs. altitude of the ABS (comparing Algorithm 1-based deployment, random deployment, and equidistant deployment).

3.6, the optimal altitudes of the ABSs are considered as 300 m, 650 m, 800 m and 1250 m for suburban, urban, dense urban and high-rise urban, respectively. Figure 3.8 shows how the coverage probability behaves with the SINR threshold. It is conspicuous that the average coverage probability of Algorithm 1 is superior to random deployment.

Figure 3.9 presents the total consumed energy for ABS movements using Algorithm 1, Algorithm 2, and naive exhaustive search, where the search is performed over all possible altitudes. Both proposed algorithms have almost similar energy consumption, while being significantly lower (9-fold saving) than the naive exhaustive search. This is due to the reduced number of ABS movements we need to perform with the proposed centralized approach. It is interesting to note that energy saving decreases from suburban to high rise urban due to the increase in the optimal altitude.

Figure 3.10 compares Algorithms 1 and 2 in terms of the maximum achievable TSE and the total consumed energy for ABS movements with different user densities in four propagation environments. One can observe that for dense networks, Algorithm 2 results in higher TSE compared to Algorithm 1. This clearly shows the advantage of altitude diversity for dense networks. Almost equal energy consumption can be observed for both algorithms. Furthermore, it can be

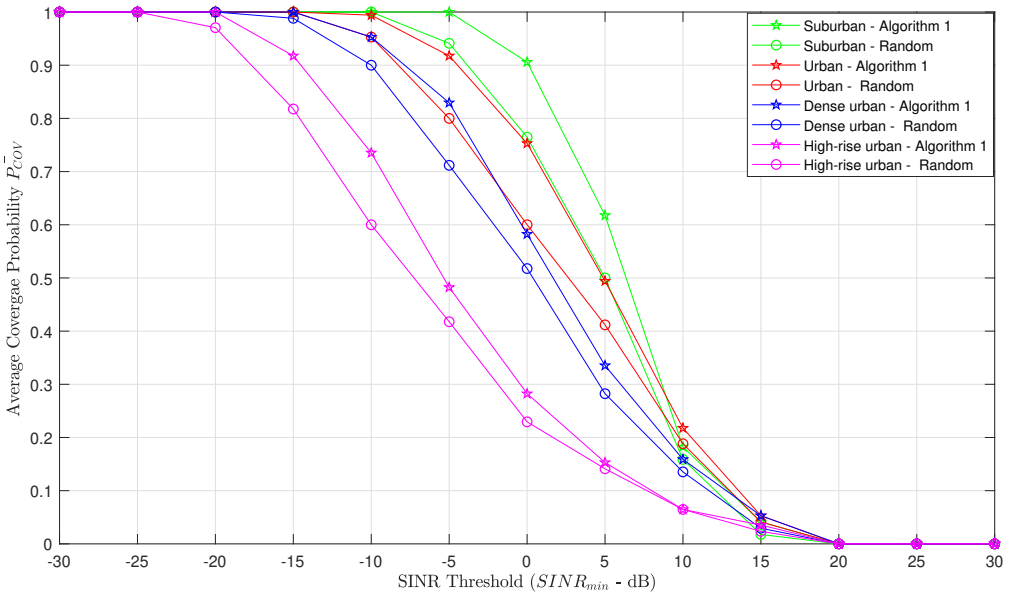

Fig. 3.8: Average coverage probability vs. Signal-to-Interference-Plus-Noise Ratio (SINR) threshold (comparison between Algorithm 1-based deployment and random deployment).

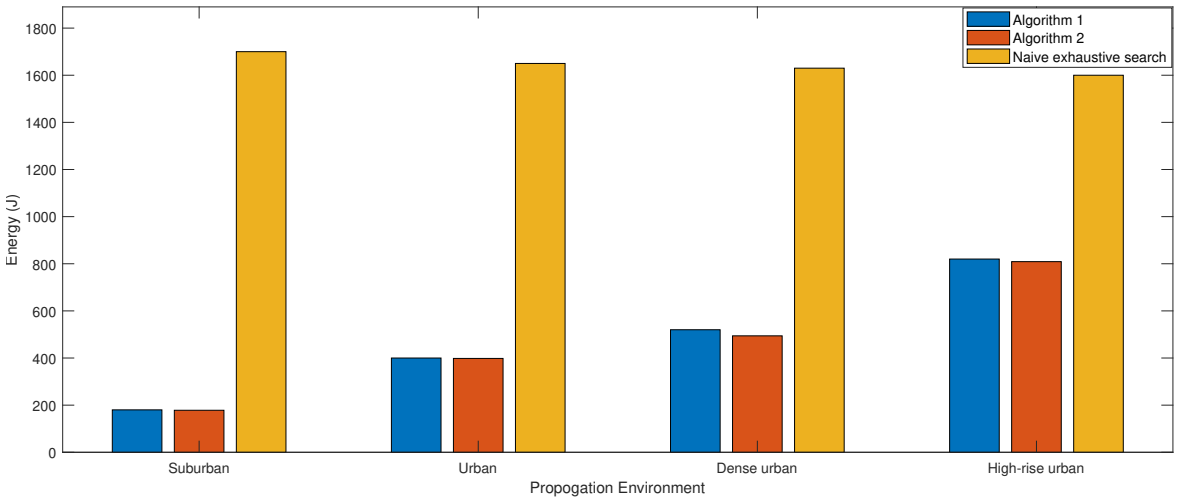

Fig. 3.9: Energy consumption of Algorithms 1 and 2 compared to naive exhaustive search.

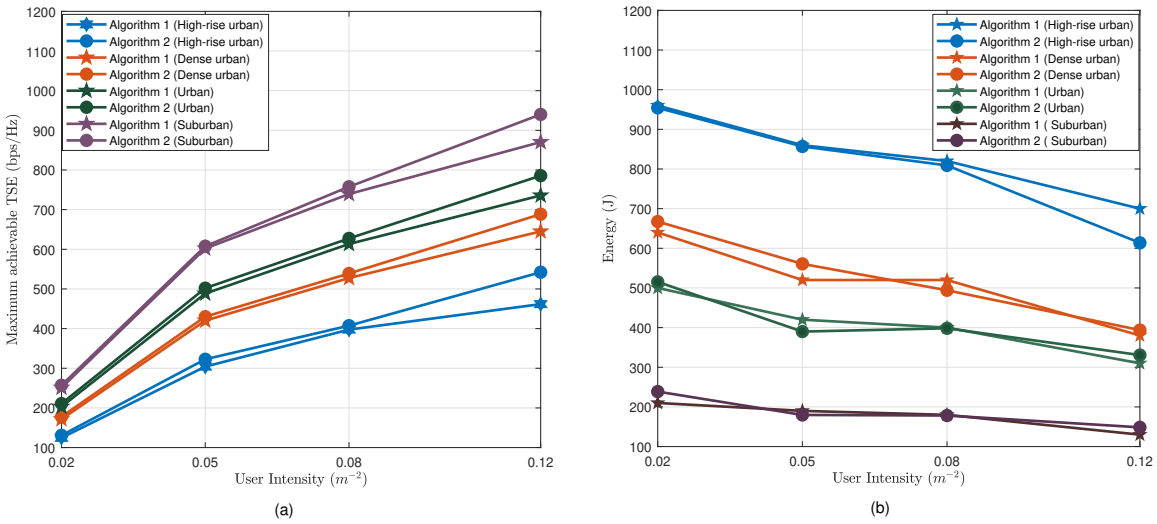

Fig. 3.10: (**a**) Maximum achievable total spectral efficiency (TSE) vs. user intensity (**b**). Energy consumption for maneuvering vs. user intensity.

observed that the total energy consumption decreases with UE density. It is clear that ABSs have to move only a small distance from the initial position to the optimal position, as in dense UE scenarios, the optimal 2D placement can be closely approximated by the uniform placement.

3.5 Conclusions

This chapter investigated the problem of ABS placement and UE assignment to maximize the sum spectral efficiency of a disaster affected wireless network. K-means clustering combined with a stable marriage problem has been used to determine the 2D placement of the ABSs and the UE assignment, while two approaches based on exhaustive search and particle swarm optimization have been proposed to determine the optimal ABS altitude. The proposed algorithms use only the statistical channel state information and the location information of the UEs and ABSs. Useful design insights such as the optimal ABS altitude, total required energy for ABS movement have been presented for different propagation environments. The proposed algorithms result in up to 8-fold saving in the energy required to maneuver the ABSs, compared to ABS deployment using naive exhaustive search.

Chapter 4

UAV Deployment in WSN System for Emergency/Remote Area Applications

4.1 Introduction

Applications of unmanned aerial vehicles (UAVs) are exponentially growing which has become an inevitable technology in various fields [1, 2]. Continuous advancement in payload capacity, complex control mechanism, energy-efficient processing and increment in flight time endurance paved the way for many other promising UAV-assisted applications. The current trend witness that the increasing interest in UAV-assisted applications in diverse verticals leads to exponential growth which is expected to be the key enabler of accomplishing the milestones of smart environment [1, 2]. UAV-assisted communication is generally divided into two categories, where the UAV acts as an aerial base station [6], or an aerial relay [7]. Potential applications of aerial base stations are supporting the overloaded terrestrial base station, providing on-demand coverage in no coverage area for special occasions and reconstructing temporary coverage in a natural disaster or an emergency situation [1, 2, 8]. They are deployed as aerial relay stations when the direct link between the source and the destination is not available or too degraded for successful communication [7, 9, 10]. On the other hand, there is an increasing interest in utilizing UAVs for data gathering applications, where they collect the data from diverse geographic regions around a city or a remote area and deliver them to a central station for analysis [1]. Notably, data collec-

tion of UAVs is getting more attention in wireless sensor network (WSN) systems.

Several applications of UAVs in WSN systems can be identified. UAVs can be used as aerial relays to collect data from the SNs deployed in remote areas, where the SNs are not able to communicate directly with the ground station (GS) [10]. Also, UAVs can be utilized to recharge SNs deployed over a large geographical area through wireless power transfer (WPT) [7]. Furthermore, UAVs can be deployed as temporary data collectors from SNs, where the dedicated GS is malfunctioning due to a natural disaster or a technical fault. In this chapter, we use UAVs as aerial relays for collecting data from remote areas. Moreover, it also can be utilized as a temporary data collector in emergencies.

Utilizing UAVs for data collection tasks can lead to several benefits. First, adjusting the altitude allows establishing strong line of sight (LoS) links to improve the channel quality. Second, UAVs' data storing and processing capabilities can be used to improve the reliability and usefulness of the collected data. This enables new cooperative communication protocols such as store-and-forward (SF) relaying [12]. Third, simple infrastructure requirements and ease of deployment make it a suitable candidate for on-demand deployment. Additionally, UAVs are maneuverable and can freely adjust their aerial positions to improve the system's performance. Also, they can utilize simultaneous wireless information and power transfer (SWIPT) techniques to recharge the SNs while collecting data.

Considering these benefits, recent research works studies the deployment of UAV in WSN systems [7, 21, 65, 66, 67, 68, 69, 64, 70, 72]. In [64], a deep reinforcement learning based mechanism is proposed such that it maximizes the amount of data collected constrained to total completion time and mobility limitations. A 3D trajectory with optimal transmit power allocation of UAV is studied in [21] such that it maximizes the system throughput. Considering the energy budget of the UAV, a unified energy management framework with wireless power transfer (WPT) and SWIPT is proposed in [7], where the UAV work in a full-duplex mode such that it minimizes the end-to-end cooperative outage probability by optimizing the UAV's power allocation parameters and the 3D trajectory. The energy efficiency of UAV in terms of propeller movement is investigated in [65, 69]. In

[65], trajectory and the sensor clustering are optimized such that it minimizes the energy consumption and maximizes the lifetime of the flying relay. The same problem as in [65] is analyzed in [69]. In contrast, they have solved in a two-step approach. Initially, a minimum number of UAVs are identified then the trajectory is optimized to minimize the overall energy consumption of the UAV. The total mission time of the UAV is considered in [67, 68, 70, 66]. In [66, 68], they have optimized the UAV's trajectory such that it minimizes the total mission time. The authors in [67] also analyze the same problem as the latter. Additionally, they have optimized sensors' transmit power such that it minimizes the overall completion time of the mission. In [72], obstacle avoiding trajectory is investigated, where the trajectory is planned such that the total mission time is minimized. The freshness of the data is investigated in [70] by introducing a new parameter called the age of information (AoI), where the trajectory of the UAV is optimized such that it minimizes the AoI of the data collected. In [71], authors have proposed a closed-form expression for the average AoI (AAoI) to estimate the optimal altitude and other parameters such that it minimizes the AAoI.

Despite the considerable contributions of the above works, there are some drawbacks considering the UAV-assisted data collection system. One of the major advantages of utilizing UAV in data collection is that it supports improving the channel strength by increasing the probability of LoS (PLOS) propagation. However, we can not always guarantee absolute LoS propagation as the LoS component's contribution depends on the UAV's position and various other environmental parameters. In contrast, authors in [64, 70, 7, 21] have considered absolute LoS propagation despite the position of the UAV and other environmental parameters, which is not feasible to achieve in actual implementation. In our work, we have considered probabilistic measure-based LoS propagation that calculates the strength of the LoS propagation based on the environmental parameters and the elevation angle. Although some of the works consider the probabilistic LoS based channel model [68, 67, 69, 72], they have failed to optimize the altitude of the UAV, which yields the trade-off between increasing LoS propagation and the pathloss. However, our work contemplates altitude optimization such that it increases system performance. Moreover, authors in [64, 70] have considered neither the probabilistic LoS model nor the altitude optimization. In [64, 70, 72, 7, 21], they have only considered a single UAV deployment which fails to analyze the on-demand and robust nature of UAV-assisted application. In contrast, we have

considered multi-UAV deployment with the relevant constraints associated with it.

Considering the air-to ground (ATG) channel model, there are no universally affirmed channel models to characterize the ATG channel. However, there are four kinds of models that have been used to characterize the GTA channels in the current literature. First, the channel model, which utilizes the exact geometrical structure of the environment and the reflective nature of the wavefront [73, 74]. Second, the empirical measurements based channel models [75, 76]. Third, pure LoS propagation which is often modeled using the free-space path loss model [64, 70, 7, 21, 77, 78]. Finally, probabilistic information-based LoS characterization is used to model the contribution of LoS and NLoS propagation [68, 69, 72, 14, 79, 63].

In our work, it is not possible to utilize geometry-based channel model as we do not have the precise geometrical structure of the environment and the reflective nature of the materials. The empirical model is also impossible because it requires access to a substantial empirical measurement database. The pure LoS propagation is often modeled as free space pathloss, where the distance is the only parameter that determines the channel strength. Thus, UAVs always try to reduce the effective distance by hovering at the minimum possible altitude. However, this is not the case in the real world deployment, where we would be able to adjust the contribution of LoS propagation by adjusting the altitude and the position of the UAV given the structure of the environment. Therefore, Considering pure LoS propagation will not help to utilize and study the benefits of altitude diversity which is one of the main advantages in UAV-assisted communication compared to terrestrial communication. The channel model that uses probabilistic information-based LoS characterization is also not exactly accurate. However, it helps to study the altitude diversity and the positioning of the UAV. All these points considered, we have utilized the probabilistic model proposed by the international telecommunication union (ITU) [80].

On the other hand, although the advanced wireless sensors are energy efficient and generally have longer battery life than conventional sensors, they should also be recharged at the appropriate period. Therefore, energy efficiency in modern WSN systems is also a critical factor. However, the energy efficiency of the

wireless sensors is not considered in the recent works [64, 70, 7, 21, 68, 69, 72]. The major reason for neglecting the energy consumption of wireless sensors in UAV-assisted data collection is that they assume the energy needed for data transmission is negligible compared to the energy needed for propeller movement. Therefore, it is considered negligible considering the system's overall energy consumption. However, this is not a fair assumption as a device's energy consumption should be compared with its own energy budget to decide its significance. Although the energy needed for transmission is negligible compared to the energy for the propeller movement, it is significant compared to the minimal energy budget of the wireless sensors. Therefore, it is crucial to consider the energy needed for the transmission and the energy efficiency of the wireless sensors.

Moreover, it is essential to realize that in WSN systems, transmit power fairness among the sensor nodes (SNs) is essential rather than the overall energy efficiency. As discussed earlier, wireless sensors are employed in larger geographical areas, where it is not feasible to recharge them often. If we only consider the overall energy efficiency of the system, there is a high chance that the energy consumption of the sensors widely varies among them. Therefore, the battery of the sensor will run out in widely varying time intervals which will create a requirement for frequent recharge operation [10]. In that case, it will not be energy efficient in terms of recharging operation as it is generally done through WPT-enabled UAVs. Considering energy efficiency with transmit power fairness will maintain the energy consumption of the sensors among them, which will help to recharge the wireless sensors roughly at the same time.

Considering all these, in this work, we are investigating a multi-UAV multi-SN system, where the SNs are randomly distributed in an area. The UAVs facilitate the collection of data from the SNs. We focus on UAV deployment with the goal of increasing the energy efficiency in the network while maintaining transmit power fairness among the SNs. The main contributions can be summarized as follows.

The key contributions of this chapter can be summarized as follows.

- The multi-UAV 3D deployment problem is divided into three subproblems such that it reduces the complexity involved in solving it as a single problem. The subproblems are UAV-SN association, 2D positioning of the UAVs and the altitude optimization of the UAVs. All three subproblems are optimized

such that the maximum transmit power among the SNs is minimized with respect to maximum power and minimum rate constraints of the SNs.

- The UAV-SN association subproblem is solved using a modified matching algorithm that customizes the Gale-Shapely algorithm to address the min-max objective problems effectively.
- A new modified pattern search (PS) algorithm is proposed for the 2D deployment of the UAVs that will utilize the prediction of descent direction, which will help for quicker convergence compared to the naive PS algorithm.
- By analyzing the nature of the altitude optimization subproblem, it is addressed through an inexact line search algorithm with Armijo and Wolfe condition that guarantees a quicker convergence than other baseline numerical optimization approaches.
- Finally, we present a combined optimization algorithm that places the approaches of all three subproblems in the suitable hierarchy such that it provides optimal or near-optimal solutions with a fewer number of iterations. At the same time, it gives the minimum number of UAVs required to serve all the SNs with the given rate and power constraints.

The chapter is structured as follows. Section 4.2 introduces the system model and the problem formulation. The proposed solution is described in Section 4.3. Section 4.4 presents the numerical results and discussion, and Section 4.5 concludes the chapter.

4.2 System Model

We consider a WSN, in which it is not feasible for the SNs to transmit directly to the GS. Thus, multiple UAVs are deployed as aerial relays to collect data from the SNs, and forward to the GS.

4.2.1 Spatial Model

As shown in Fig. 4.1, a set of K energy constrained wireless SNs (denotes as $\mathcal{S}$) is randomly distributed in the area of interest. A set of L UAVs (denoted as $\mathcal{U}$) is deployed to collect the data and forward it to the nearby GS. The UAVs are

controlled by the GS. Initially, the GS deploys the minimum required number of UAVs based on the maximum user capacity of a UAV. Therefore, we have

$$L = \left\lceil \frac{K}{N_{\max}} \right\rceil, \tag{4.1}$$

where $\lceil . \rceil$ denotes the ceiling function, and $N_{\max}$ is the maximum number of nodes a UAV can serve.

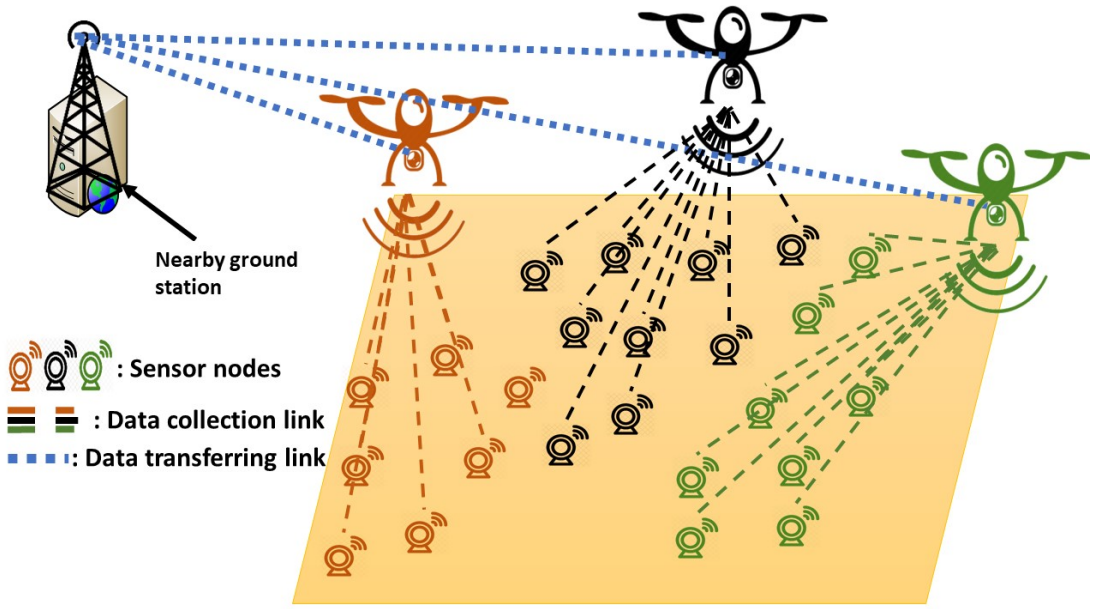

Fig. 4.1: The data gathering and data transferring links and the spatial distribution of SNs, UAVs, and the GS.

The position of the l^{th} UAV in the 3-dimensional (3D) space is denoted by W_l, where $W_l = (x_l, y_l, H_l)$, x_l and y_l are the ground coordinates, and H_l is the altitude. The set of all UAV locations is denoted by $\mathcal{W} = \{W_1, \ldots, W_L\}$. As the SNs are deployed on the ground, the location of the k^{th} SN is denoted as $Q_k = (a_k, b_k, 0)$, where a_k and b_k are the ground coordinates of the k^{th} SN. Also, we define $\mathcal{Q} = \{Q_1, \ldots, Q_K\}$, which is the set containing location information of all SNs. The location of the GS is denoted as $X_{gs} = (x_{gs}, y_{gs}, H_{gs})$. x_{gs} and y_{gs} are the ground coordinates, and H_{gs} is the height of GS. We denote the set of SNs connected to the l^{th} UAV with ψ_l. Also, the set $\Psi = \{\psi_1, \ldots, \psi_L\}$ specifies the complete user association. It is important to note that the elements of Ψ are disjoint, thus a particular SN can be associated with only one UAV.

4.2.2 Channel Model

Two types of wireless links are found in the system, namely, the data transferring links (DTLs), and the data collection links (DCLs). The DTLs represent UAV-GS communications. Considering the height of the GS antennas and the altitude of the UAVs, the DTLs can be identified as air-to-air (ATA) links. Due to the absence of scatterers in ATA links, the impact of multipath components on the received signal power is negligible. Therefore, small-scale fading effect can be neglected, and the ATA links can be accurately modeled using free-space path loss model (FSPL). The power gain of the DTL channel between l^{th} UAV and the GS is given by

$$h_{l,gs} = \frac{G_1}{\|H_l - H_{gs}\|^2 + \|x_l - x_{bs}\|^2 + \|y_l - y_{bs}\|^2}, \tag{4.2}$$

where $G_1 = g_t g_r \left(\frac{\lambda}{4\pi d_0}\right)^2$, λ is the wavelength of the carrier signal, $d_0 = 1$ m, g_t and g_r are the antenna gains of the UAV and the GS, respectively. The achievable rate of the l^{th} DTL is given by

$$R_{l,gs} = B_c \log_2 \left[1 + \frac{P_{u,l} h_{l,gs}}{B_c N_0}\right], \tag{4.3}$$

where B_c is the allocated channel bandwidth, p_l^u is the transmit power of the l^{th} UAV and N_0 is the power spectral density of the Gaussian noise.

The DCLs represent the links between the SNs and the UAVs, which are often referred to as ground-to-air (GTA) links. They exhibit similar characteristics as their reciprocal ATG link. Generally, ATG links experience both LoS propagation or NLoS propagation, depending on the position of the aerial device, ground device, and the environmental parameters. To make our system model more general, we refer to the probabilistic model for ATG links proposed by the ITU [80]. For simplicity, without loss of generality, we use the simplified ITU model proposed in [14]. The probability of having a LoS DCL between the k^{th} SN and the l^{th} UAV is given by

$$p_{LoS}(\theta_{l,k}) = \frac{1}{1 + \sigma e^{-\beta[\theta(l,k) - \sigma]}}, \tag{4.4}$$

where $\theta(l,k)$ is the elevation angle between the k^{th} SN and the l^{th} UAV and β and σ are the environmental parameters which represent the geometrical structure of the environment. As the time taken to move a UAV is significantly larger than the

typical coherence time of a wireless channel, it is not feasible to use instantaneous channel state information (CSI) for the user association and UAV placement, as it may lead to a solution based on outdated CSI. Therefore, we consider the average channel power gain, where the effect of small-scale fading is averaged out. For brevity, hereafter, we refer to it as the channel power gain. The channel power gain between the k^{th} SN and the l^{th} UAV is modeled as [6, 82]

$$\bar{h}_{\text{w}}(l,k) = \frac{G_w}{\sqrt{H_l^2 + \|x_l - a_k\|^2 + \|y_l - b_k\|^2}^{\alpha_w}} \ , \tag{4.5}$$

where the subscript $w \in \{LS, NS\}$ such that LS and NS denote LoS and NLoS scenarios, α_w is the path loss exponent,

$$G_w = \mathbb{E}\left[|\nu_w|^2\right] g_l g_k \left(\frac{\lambda}{4\pi}\right)^{\alpha_w} \tag{4.6}$$

with g_l and g_k being the antenna gains of the UAV and the SN, ν_w is the small-scale fading amplitude, and $\mathbb{E}[.]$ denotes the expectation, respectively. Note that $\alpha_{LS} < \alpha_{NS}$. It is assumed that $|\nu_{LS}|$ follows a Rician distribution with K-factor κ, while $|\nu_{NS}|$ follows a Rayleigh distribution. Using (4.4) and (4.5), the effective channel power gain between the k^{th} SN and the l^{th} UAV is given as [63]

$$\bar{h}_{l,k} = p_{LoS}(\theta_{l,k})\bar{h}_{\text{LS}}(l,k) + (1 - p_{LoS}(\theta_{l,k}))\bar{h}_{\text{NS}}(l,k) \ . \tag{4.7}$$

We assume that each UAV is equipped with directional antennas such that the coverage region is limited to a cone with a fixed radius on the ground plane. Furthermore, we assume that orthogonal channels are allocated to each UAV for DCLs, eliminating inter-cluster interference. Within a cluster, each UAV adopts a frequency division multiple access (FDMA) technique, and designates a dedicated channel to each SN. Thus, intra-cluster interference also can be neglected. Therefore, the average achievable rate of the DCL between the k^{th} SN and the l^{th} UAV is given by

$$R_{l,k} = B_0 \log_2\left[1 + \frac{P_{s,k}\bar{h}_{l,k}}{B_0 N_0}\right] \ , \tag{4.8}$$

where B_0 is the allocated channel bandwidth and $P_{s,k}$ is the transmit power of the k^{th} SN.

4.2.3 Problem Formulation

In this chapter, our aim is to improve the energy efficiency of the SNs by reducing the transmit power required to achieve a given rate requirement, while maintaining fair energy consumption among all SNs. Therefore, our objective is to optimize the 3D location of the UAVs, and associate the SNs to UAVs such that the maximum transmit power among the SNs to achieve a given rate threshold is minimized. The transmit power at the k^{th} SN is written using (4.8) as

$$P_{s,k} = \frac{N_0}{\bar{h}_{l,k}} \left(2^{\frac{R_2^{th}}{B_0}} - 1 \right). \tag{4.9}$$

The optimization problem can be formally stated as

P :

$$\underset{\mathcal{W},\,\Psi}{\text{minimize}} \quad P_0 = \max_{k \in \mathcal{S}} P_{s,k} \tag{4.10a}$$

$$\text{subject to} \quad P_0 \leq P_{s,max}, \forall k \in \mathcal{S}, \tag{4.10b}$$

$$P_{u,l} \leq P_{u,max}, \forall l \in \mathcal{U}, \tag{4.10c}$$

$$R_{l,gs} \geq R_1^{th}, \forall l \in \mathcal{U}, \tag{4.10d}$$

$$R_{l,k} \geq R_2^{th}, \forall k \in \mathcal{S}, \forall l \in \mathcal{U}, \tag{4.10e}$$

$$H_l \geq H_{min}, \forall l \in \mathcal{U}, \tag{4.10f}$$

$$\psi_j \cap \psi_i = \emptyset, \quad \forall i \neq j \in \mathcal{U}, \tag{4.10g}$$

$$|\psi_l| \leq N_{max} \quad \forall l \in \mathcal{U} \ , \tag{4.10h}$$

where R_1^{th} and R_2^{th} are the minimum rate requirements of a DTL and a DCL, respectively. Also, $P_{u,max}$ and $P_{s,max}$ are the maximum allowed transmit power of the UAVs and the SNs respectively. The constraint (4.10b) ensures the transmit powers of SNs do not exceed P_0 at the same time P_0 does not exceed the maximum transmit power constraint, while (4.10c) incorporate the maximum transmit power constraint of a UAV. Constraints (4.10d) and (4.10e) represent the minimum rate requirements imposed on the links. The minimum altitude constraint of a UAV is given as (4.10f), while (4.10g) reflects disjoint association of SNs to UAVs. Furthermore, (4.10h) imposes a constraint on the maximum number of SNs that can be associated to a single UAV.

Given the channel bandwidth B_0, and the minimum rate requirement R_2^{th}, the objective function and (4.10b) can be re-written as $\max_{k\in\mathcal{S}} \quad \frac{C_0}{\bar{h}_{l,k}}$, and $P_{s,max} \geq P_{s,k}, \forall k \in \mathcal{S}$ respectively, where $C_0 = N_0 \left(2^{\frac{R_2^{th}}{B_0}} - 1\right)$.

Since C_0 is a constant, it is interesting to note that the original problem can be transformed to a problem of maximizing the channel power gain of the worst channel power gain user. Therefore, we can rewrite the the problem as

P_{mod} :

$$\underset{\mathcal{W},\,\Psi}{\text{maximize}} \quad \min_{k\in\mathcal{S}} \quad \bar{h}_{l,k} \ , \tag{4.11a}$$

$$\text{subject to} \quad P_{s,max} \geq P_{s,k}, \forall k \in \mathcal{S} \tag{4.11b}$$

where the other constraints remain unchanged from the original problem P. Hereafter, we consider solving the transformed problem P_{mod}.

4.3 Proposed Solution

In this section, we present our proposed algorithm to solve the problem P_{mod}. One can observe that P_{mod} is a non-convex problem. Moreover, it is an NP-hard problem, as finding Ψ can be reduced to a well known Boolean satisfiability problem, which cannot be solved with polynomial complexity. This makes joint optimization over $\mathcal{W}$ and Ψ computationally intensive. To obtain a solution with a reasonable computational effort, we divide the problem into three subproblems, and apply alternative optimization to each subproblem, iteratively. We consider three subproblems, namely, UAV-SN association ($P1$), UAV 2D positioning($P2$), and UAV altitude selection ($P3$) subproblems. The overall concept of the proposed algorithm is illustrated as flowchart in Fig. 4.2. The sections related to the respective subproblem is highlighted with dashed line boxes with the respective label of the subproblem.

4.3.1 UAV-SN association subproblem

In this subproblem, we fix the locations of the UAVs, and associate the SNs with the UAVs such that the minimum channel power gain experienced by an SN is

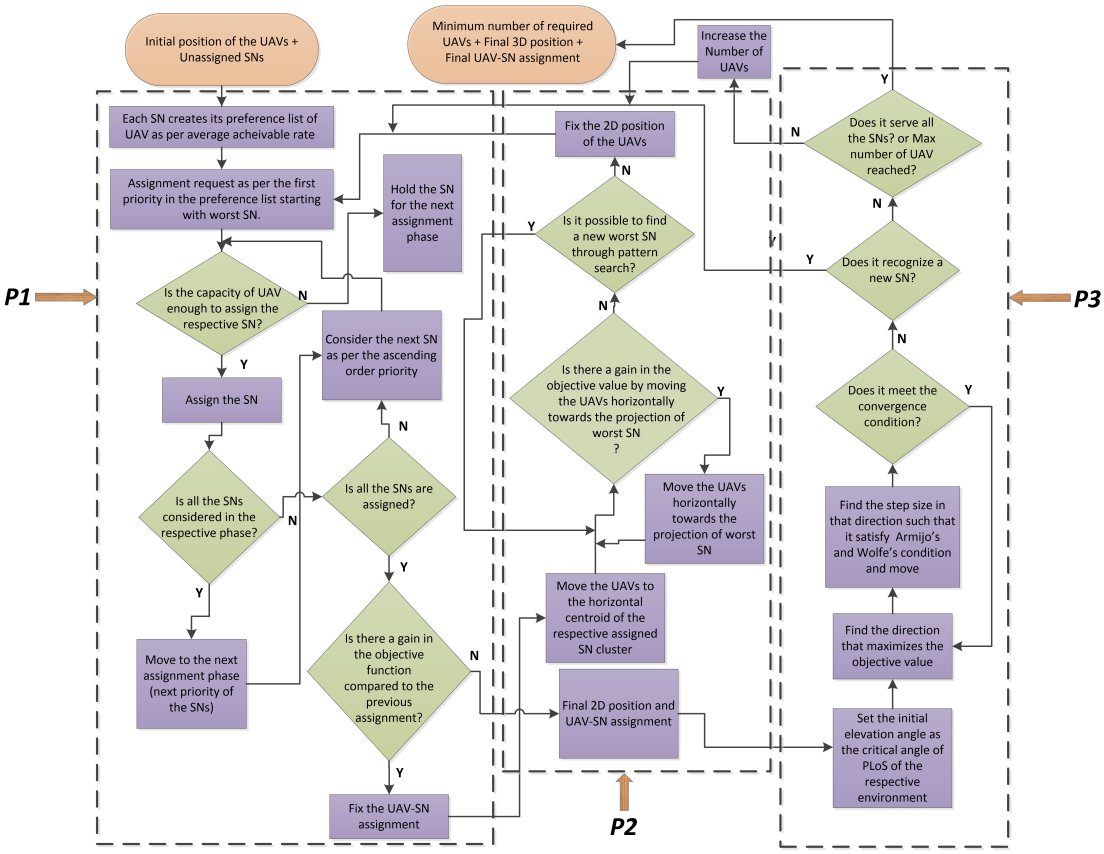

Fig. 4.2: Flowchart of our proposed algorithm . Dashed line boxes differentiate the approaches related to the subproblems

maximized, as per P_{mod}. The optimization problem can be written as

$P1$:

$$\underset{\Psi}{\text{maximize}} \quad \min_{k \in \mathcal{S}} \quad \bar{h}_{l,k} \tag{4.12a}$$

$$\text{subject to} \quad P_0 \leq P_{s,max}, \forall k \in \mathcal{S}, \tag{4.12b}$$

$$\psi_j \cap \psi_i = \emptyset, \quad \forall i \neq j \in \mathcal{U}, \tag{4.12c}$$

$$|\psi_l| \leq N_{max} \quad \forall l \in \mathcal{U} \tag{4.12d}$$

User association problems can be reduced to the well-known knapsack problem, an NP-hard problem which can not be solved in polynomial time. Therefore, the problems of this nature are generally addressed by matching algorithms [27, 81, 87]. We model $P1$ as a stable marriage problem, and propose a modified Gale–Shapley algorithm to obtain a SN-UAV association which ensures transmit power fairness. Initially, a priority list is created using the achievable channel

power gains as the weights. Since conventional Gale–Shapley algorithm fails to establish fairness among the connections, we propose a novel SN association algorithm to ensure transmit power fairness.

In the modified user association algorithm, the first connection priority will be assessed considering the weights of the first preference level. For that, it will create a matrix that represents the connection priority of the non-connected SNs considering the average achievable rate as the weights ($\mathbb{P}^{\mathrm{SN}}$). In $\mathbb{P}^{\mathrm{SN}}$, each column will represent a SN. In the first round of connection, we consider the first row (highest priority of the SNs) of $\mathbb{P}^{\mathrm{SN}}$ and order them in ascending manner assessing the weights denoted as $\mathcal{P}_1$. As our objective is max-min in nature we do the connection as per $\mathcal{P}_1$ where the SN with lower weights will be given the higher priority. The main motivation for the proposed approach is if we connect the SNs through the typical connection order, there is a high probability that the SN which has the worst weight will not be able to connect to its first priority UAV. Therefore, it should connect to its next priority UAV, which leads to higher transmit power usage. This results in an unfair situation in terms of the life time of the SNs. This can be prevented by allowing the SNs which

Algorithm 3: UAV-SN assignment algorithm

Data: $\mathcal{W}$, $\mathcal{Q}$
Result: Ψ
begin
  Block-A
    $N_l^C \Leftarrow$ Number of SNs connected to l^{th} UAV
    $[\mathbb{P}^{\mathrm{SN}}]_{L\times K} \Leftarrow$ Priority matrix of non-connected SNs
    $l = 1$
    while $\left|\mathbb{P}^{SN}\right| \neq 0$ **do**
      $\mathcal{P}_l \Leftarrow$ Ascending Ordered vector of SNs as per l^{th} priority (row) of $\mathbb{P}^{\mathrm{SN}}$
      for $i = 1, \ldots, |\mathcal{P}_l|$ **do**
        $e = \mathcal{P}_l(i) \Leftarrow (k+1)^{\text{th}}$ UAV preference of i^{th} SN
        if $N_e^C \leq N_{max}$ *and* $i \notin \Psi$ **then**
          $i \in \psi_e$
          $N_e^C = N_e^C + 1$
      $\mathbb{P}^{\mathrm{SN}} \Leftarrow$ Remove the rows respective to the connected SNs and recreate the matrix only with non-connected SNs.
      $l = l + 1$
    $\Psi^* = \{\psi_l\}_{l=1}^{L}$

have smaller weights, to connect to their respective preference UAV. For better clarity, we have compared the proposed algorithm with the conventional matching algorithm through an example scenario given below.

Once priority list is created as per UAV's and SN's preference, the conventional Gale–Shapley algorithm will associate SNs, starting from the SN which has the highest weight in its first priority , while cross checking with UAV's preference, and proceed in the descending order until all the SNs are associated, such that the SN with the lowest weight in the first priority will be connected last. It is clear that this approach fails to establish fairness among the SNs, as the SN with the worst channel is associated last, and the transmit power required to maintain the rate threshold will be higher compared to the other SNs. Therefore, we propose a novel SN association algorithm to ensure transmit power fairness. For better clarity, we have compared the proposed algorithm with the conventional matching algorithm through an example scenario.

Consider a network with $K = 9$ SNs and $N_{\max} = 3$. The link weights of each SN to the available UAVs are given in List 1, where the i^{th} column represents the ordered channel power gains of the i^{th} SN to each UAV. List 2 shows the corresponding UAV that provides the weights in List 1. In here, the high-rise urban environment is considered.

SNs	1	2	3	4	5	6	7	8	9
Weights / 10^{-7}	40	41	36	38	37	33	42	35	34
	28	29	26	34	35	25	27	24	31
	10	19	20	21	27	13	26	11	25

List 1: Weight of the priorities of each sensor

SNs	1	2	3	4	5	6	7	8	9
UAV	2	2	1	2	2	2	2	3	3
	1	1	3	3	3	3	1	1	2
	3	3	2	1	1	1	3	2	1

List 2: The respective UAV preference for the weight in List 1

If the conventional Gale–Shapley algorithm is applied, it will consider the first

row of List 1 and give the connection priority to the SN, which has the highest weight, and proceed in the descending order of the weights. If all the SNs are not connected in the first phase based on first preference, it will consider the second preference in the descending order for the second phase. This will be repeated until all the SNs are associated. Therefore, the order of association of the SNs will be 7, 2, 1, 3, 8, 9, 5, 4 and 6. The resulting channel power gains are shown in Fig. 4.3.

SNs	1	2	3	4	5	6	7	8	9
Weights / 10^{-7}	40	41	36	38	37	33	42	35	34
	28	29	26	34	35	25	27	24	31
	10	19	20	21	27	13	26	11	25

The fill color represents the connected UAV as given below.

UAV 1 UAV 2 UAV 3

Fig. 4.3: UAV-SN assignment through conventional gale-shapely algorithm

In Algorithm 3, the first connection phase also considers the first row of List 1. However, the priority will be given to the SN which has the smallest weight, and proceed in the ascending order of the weights. If all the SNs are not associated in the first phase, it will consider the second row for the second phase. This will be repeated until all the SNs are associated. If it reaches the last phase, the remaining SNs will be connected to the respective UAVs. The order of association for the SNs will be 6, 9, 8, 3, 5, 4, 7, 1 and 2. The resulting channel power gains are shown in Fig. 4.4.

SNs	1	2	3	4	5	6	7	8	9
Weights / 10^{-7}	40	41	36	38	37	33	42	35	34
	28	29	26	34	35	25	27	24	31
	10	19	20	21	27	13	26	11	25

The fill color represents the connected UAV as given below.

UAV 1 UAV 2 UAV 3

Fig. 4.4: UAV-SN assignment through Algorithm 3

In Algorithm 3-b (discussed in section 4.4), the first connection phase considers the second row of List 1. The priority will be given to the SN which has the smallest weight, and proceed in the ascending order of the weights. If all the SNs are not associated in the first phase, it will consider the third row weights for the second phase priority. This will be repeated until all the SNs are associated. In any case, if it reaches the last phase with remaining assignments it will connects the SNs to its last priority where order does not matter.The order of association for the SNs will be 8, 6, 3, 7, 1, 9, 2, 4 and 5. The resulting channel power gains are shown in Fig. 4.5.

SNs	1	2	3	4	5	6	7	8	9
Weights / 10^{-7}	40	41	36	38	37	33	42	35	34
	28	29	26	34	35	25	27	24	31
	10	19	20	21	27	13	26	11	25

The fill color represents the connected UAV as given below.

UAV 1 UAV 2 UAV 3

Fig. 4.5: UAV-SN assignment through Algorithm 3-b

The utilities of the worst user with the conventional Gale–Shapley algorithm, Algorithm 3 and Algorithm 3-b are 13×10^{-7}, 19×10^{-7} and 27×10^{-7} respectively. It is clear that for this example, Algorithm 3 and Algorithm 3-b results in a 46% and 107% better channel compared to the conventional approach.

4.3.2 2D positioning subproblem

In this subproblem, we fix the altitudes of the UAVs and the UAV-SN association, then find the 2D positions of the UAVs such that the minimum channel power gain experienced by an SN is maximized, as per P_{mod}. The optimization problem can be written as

$P2:$

$$\underset{x_l, y_l : \forall l \in \mathcal{U}}{\text{maximize}} \quad \min_{k \in \mathcal{S}} \quad \bar{h}_{l,k} \tag{4.13a}$$

$$\text{subject to} \quad P_0 \leq P_{s,max}, \forall k \in \mathcal{S}, \tag{4.13b}$$

$$P_{u,l} \leq P_{u,max}, \forall l \in \mathcal{U}., \tag{4.13c}$$

$$R_{l,gs} \geq R_1^{th}, \forall l \in \mathcal{U}, \tag{4.13d}$$

$$R_{l,k} \geq R_2^{th}, \forall k \in \mathcal{S} \tag{4.13e}$$

As our objective is maintaining transmit power fairness, we aim to maximize the minimum average channel gain among the SNs. Therefore, we propose a modified PS algorithm that achieves faster convergence in max-min objective problems, compared to the naive PS algorithm.

In the proposed modified PS algorithm, as it is mentioned in the flowchart in Fig. 4.2, the initial position of a UAV is set to the horizontal centroid of SN cluster associated in $P1$, projected to the plane of the UAV. Each UAV then identifies the SN which has the minimum channel power gain (referred to as the "worst SN") in the respective cluster k_0^l. Then move the UAVs towards the direction of the SN worst SN, until an increase in the channel power gain is observed for the worst SN ($\delta G_0 > 0$), or any other SN achieves a lower channel power gain than the current worst SN. Next, a naive PS will be conducted in the vicinity of the final position to find whether there exist a new worst SN within the cluster. These two processes will iteratively run until the PS cannot find a new worst SN inside the cluster ($\delta G_0 = 0$). The converging positions of the UAVs are considered as the best 2D positions for the given UAV-SN association identified in $P1$, and the current altitudes of the UAVs. These ideas are formally stated in Algorithm 4 as well as in the flowchart. Since the PS is performed only in the vicinity of the worst SN, faster convergence is achieved compared to the naive PS approach used in [81].

The problem similar to $P2$ in a multi-UAV system is generally addressed through a clustering algorithm along with a matching algorithm, where both the algorithms will be used iteratively, until the convergence condition is met [6, 81, 27]. These approaches are mainly used when the objective is sum utility

Algorithm 4: 2D positioning of the UAVs - Modified Pattern Search (MPS)

Data: $\mathcal{Q}$, Ψ, $H_l \quad \forall l \in \mathcal{U}$
Result: $\mathbf{q}_l^* = (x_l^*, y_l^*) \quad \forall l \in \mathcal{U}$, g_s
begin
  for $l = 1, \ldots, L$ **do**
    $i = 1 \Leftarrow$ Iteration index
    $\mathbf{q}_l(1) \Leftarrow$ UAV's initial 2D position is set as the centroid of nodes coordinate
    Initialize Δ value,
    $k_0^l = \arg\min_{k \in \psi_l} \quad \bar{h}_{l,k}$
    $r(k_0^l) \Leftarrow$ 2D position of k_0^l SN
    $G_0(q) \Leftarrow$ Returns the channel power gain of the k_0^l node in the l^{th} UAV's position $q_l(i)$
    $\delta G_0 \Leftarrow$ gain achieved comparing to the previous position
    Set δG_0 to a postive value
    $\mathbf{q}_{tem} = \mathbf{q}_l(1)$
    $\gamma \Leftarrow$ Number of iteration defined for convergence
    $j = 1 \Leftarrow$ Iteration index to check the data transferring rate constraint
    while $i < \gamma$ **do**
      while $\delta G_0 > 0$ **do**
        $\mathbf{q}_v^l(j) = \mathbf{q}_{tem}$
        $\eta^l(j) = logical(R_{l,gs} \geq R_1^{th}) \times \bar{h}_{l,k}$
        $\mathbf{q}_{tem} = \mathbf{q}_{tem} + \frac{\mathbf{q}_{tem} - r(k_0^l)}{\|\mathbf{q}_{tem} - r(k_0^l)\|}\Delta$
        Calculate δG_0
        if $\delta G_0 > 0$ **then**
          $j = j + 1$
      Block-B : naive pattern search
        $q^1 = x_u + \Delta, y_u$, $q^2 = x_u - \Delta, y_u, y_u$, $q^3 = x_u, y_u + \Delta, y_u$, $q^4 = x_u, y_u - \Delta$
        $G_0^1 = G_0(q^1), G_0^2 = G_0(q^2),, G_0^3 = G_0(q^3), G_0^4 = G_0(q^4)$ $\mathcal{G} = [G_0^1, G_0^2, G_0^3, G_0^4]$
        Calculate δG_0 for $\max\{\mathcal{G}\}$
      if $\delta G_0 > 0$ **then**
        $j = j + 1$
        Go to **Block-A**
      Reduce Δ
      $i = i + 1$
    $f = \arg\max_{j \in \mathcal{J}^l} \quad \eta^l(j)$
    $g_c(l) = \max_{j \in \mathcal{J}^l} \quad \eta^l(j)$
    $\mathcal{J}^l \Leftarrow$ Set of iterations in the l^{th} UAV positioning
    $\mathbf{q}_l^* = \mathbf{q}_v^l(f)$
  $g_s = \min_{r \in \mathcal{U}} \quad g_c(r)$

maximization. In [81], the authors have considered UAV placement through naive PS algorithm, which focuses on sum utility maximization objective. Therefore, it fails to maintain fairness among the SNs (Users), which is crucial in systems like UAV-assisted data collection.

4.3.3 Altitude selection subproblem

In this subproblem, we fix the 2D positions of the UAVs and the UAV-SN association, then find the altitude of the UAVs such that the minimum channel power gain experienced by an SN is maximized, as per P_{mod}. The optimization problem can be written as

$P3:$

$$\begin{aligned}
\underset{H_l : \forall l \in \mathcal{U}}{\text{maximize}} \quad & \min_{k \in \mathcal{S}} \quad \bar{h}_{l,k} && \text{(4.14a)}\\
\text{subject to} \quad & P_0 \leq P_{s,max}, \forall k \in \mathcal{S}, && \text{(4.14b)}\\
& P_{u,l} \leq P_{u,max}, \forall l \in \mathcal{U}, && \text{(4.14c)}\\
& R_{l,gs} \geq R_1^{th}, \forall l \in \mathcal{U}, && \text{(4.14d)}\\
& R_{l,k} \geq R_2^{th}, \forall k \in \mathcal{S}, && \text{(4.14e)}\\
& H_l \geq H_{min}, \forall l \in \mathcal{U}. && \text{(4.14f)}
\end{aligned}$$

In $P2$, the objective is to maximize the rate of the worst SN. When the 2D positions of the UAVs change, the worst SN also changes within the optimization process. However, as we have shown below, the worst SN within a cluster does not change when we adjust the UAV altitudes. Furthermore, the objective function is continuous and differentiable with respect to the elevation angle equivalently the UAV altitude. Therefore, $P3$ can be solved with a different approach compared to $P2$.

Consider the l^{th} SN cluster, which is served by l^{th} UAV. The worst SN is denoted by k_0^l

$$k_0^l = \arg\min_{k \in \psi_l} \quad \bar{h}_{l,k}. \tag{4.15}$$

Given the 2D positions and the the UAV-SN associations are fixed, the below conditions hold true

$$\theta(l, k_0^l) \leq \theta(l, i) \; ; \forall i \in \psi_l \tag{4.16}$$

$$zd(l, k_0^l) \geq d(l, i) \; ; \forall i \in \psi_l \; , \tag{4.17}$$

where $d(l, i)$ represents the horizontal distance between the l^{th} UAV and the i^{th} SN. Conditions (4.16) and (4.17) will remain true regardless of the altitude of the l^{th} UAV. This is valid for all clusters. Therefore, the worst SN will not change in the altitude optimization process.

As per (4.14a), the objective function related to the altitude optimization of the i^{th} cluster is given in (4.18), where $k = k_0^l$. In (4.14a), the altitude of the UAV H_l is represented by the elevation angle $\theta(l, k)$, as $d(l, i)$ is constant for a given cluster, since $H_l = d(l, k) \tan(\theta(l, k))$. The objective function contains contributions of LoS and NLoS propagation. When the elevation angle is increased, the probability of NLoS propagation decreases. Furthermore, since the link length increases with $\theta(l, k)$, the path loss also increases. Therefore, the contribution of the NLoS component always decreases with the elevation angle, hence decreases with the UAV altitude. To this end, the NLoS component can be neglected from the altitude optimization problem. On the other hand, the LoS component exhibits both increasing and decreasing behaviors with the elevation angle, accounting for the existence of maximas of the objective function.

The first derivative of the LoS component with respective to the elevation angle is given in (4.19). Due to the complicated mathematical form of (4.19), it is not feasible to find an analytical solution for $\frac{\partial\, h_{LoS}(l,k)}{\partial\, \theta(l,k)} = 0$, to obtain the stationary points which leads to the optimal elevation angle. Although, the constraints (4.14b)-(4.14f) are convex, the objective function is neither convex nor concave, as the second derivative of (4.14a) is not strictly negative nor positive. Therefore, this optimization can not be addressed through general convex optimization techniques.

We resolve to numerical optimization techniques to obtain a solution for $P3$.

Generally, global optimality is not guaranteed with numerical optimization techniques. However, a local optimum can be obtained with a reasonable computational complexity. Considering this, we analyze the behavior of the objective function to gain insights to develop a numerical solution for $P3$.

Two factors determine the contribution of the LoS component to the channel power gain. First is the PLOS, and the other is the pathloss. An increment PLoS increases the channel power gain, while an increment in pathloss decreases the channel power gain. The effective channel power gain will be determined by the relative contribution of these two factors. The pathloss increases exponentially with the elevation angle (4.18). On the other hand, PLoS displays a sigmoid behavior (4.4), where it remains almost constant with $\theta(l,k)$ initially, then a steep increment, followed by a saturation region. Considering these two behaviors, if pathloss dominates for smaller $\theta(l,k)$, it will dominate throughout the other angle as it increases exponentially with the angle. In such a scenario, the lowest angle is the one that gives better gain. However, if PLoS dominates initially, at some point the pathloss will start to dominate, as PLoS strength will saturate. Once the pathloss starts to dominate, LoS will not dominate again, as pathloss increases exponentially with $\theta(l,k)$, while the contribution of the LoS component is saturating. These intuitive analyses guarantee that although this is not a convex function, it only has one stationary point (maxima) within the range. Therefore, if one approach can guarantee the local maxima, it is sufficient for the altitude optimization, as the solution is highly likely to be the global optimum.

$$\bar{h}_{l,k} = \underbrace{\frac{1}{1+\sigma e^{-\beta[\theta(l,k)-\sigma]}} \frac{G_{LS}}{\sqrt{d(l,k)^2\left(1+\tan^2\left(\theta(l,k)\right)\right)}^{\alpha_{LS}}}}_{\bar{h}_{\mathrm{LS}}(l,k)} + \underbrace{\left(1-\frac{1}{1+\sigma e^{-\beta[\theta(l,k)-\sigma]}}\right) \frac{G_{NS}}{\sqrt{d(l,k)^2\left(1+\tan^2\left(\theta(l,k)\right)\right)}^{\alpha_{NS}}}}_{\bar{h}_{\mathrm{NS}}(l,k)} \tag{4.18}$$

We employ line search optimization which is a widely used numerical optimization method [83, 84], because with the selection of suitable line search method and the parameters, convergence to a local optimal solution is guaranteed. There

$$\frac{\partial\, \bar{h}_{\mathrm{LS}}(l,k)}{\partial\, \theta(l,k)} = \frac{\sigma\beta G_{LS} e^{-\beta(\theta(l,k)-\sigma)} \left(d(l,k)^2 \left(\tan^2(\theta(l,k))+1\right)\right)^{-\alpha_{LS}/2}}{\left(\sigma e^{-\beta(\theta(l,k)-\sigma)}+1\right)^2} - \frac{\alpha_{LS} d(l,k)^2 G_{LS} \tan(\theta(l,k)) \sec^2(\theta(l,k)) \left(d(l,k)^2 \left(\tan^2(\theta(l,k))+1\right)\right)^{-1-\alpha_{LS}/2}}{\sigma e^{-\beta(\theta(l,k)-\sigma)}+1} \tag{4.19}$$

are two main types of line search optimization, based on how the step sizes are chosen, namely, exact line search, and inexact line search. In exact line search, the step size is chosen by solving an optimization problem, such that it provides the steepest descent in the selected descent direction. In our case, the optimization problem that should be solved to find the optimal step size has the same complexity as our original optimization problem $P3$. Therefore, we follow the inexact line search which intelligently chooses the step size based on the available information such as the value of the objective function, and the first derivative of it at the current solution.

Two main challenges must be overcome in inexact line search to guarantee the convergence to an optimal point. First, we should avoid decreases in the function value which are smaller compared to the step length. Second, we should ensure that the step size is not too small compared to the initial rate of decrease. If either of the above happens, the optimization process oscillates without converging to an optimal point. To tackle both the challenges, we apply Armijo's condition and Wolfe's condition [85]. They are generally defined for minimization problems. To maintain the consistency with previous subproblems, we keep $P3$ as a maximization problem. Therefore, we apply necessary modifications to the Armijo's condition and Wolfe's conditions such that they can be utilized in a maximization problem.

4.3.4 Overall Optimization Process

Let the value of the objective function in the i^{th} iteration as

$$f(\Theta_i) = h_{LoS}(l,k)\,[i]\,, \tag{4.20}$$

Algorithm 5: Altitude Optimization

Data: $x_l, y_l \quad : l \in \mathcal{U}, \mathcal{Q}, \Psi$
Result: $H_l^* \quad l \in \mathcal{U}$
$\varepsilon_0 = 0$
$i = 0 \Leftarrow$ Iteration index.
Set $\varepsilon_0 = \theta_c$
$\theta_c = \arg\max_{\theta \in \{0,90\}} \quad PLoS'(\theta)$
while $f'(\Theta_i) > \varrho$ *and* $\Theta_i \geq \theta_{min}$ *and* $\eta_2 = true$ **do**
  $\theta_{min} \Leftarrow$ elevation angle for respective minimum altitude constraint.
  $\varrho \Leftarrow$ Minimum rate of change defined for convergence
  while $[(4.22) and (4.23)] = false$ **do**
    $\Theta_{i+1} = \Theta_i + \varepsilon_i g_i$
    $\varepsilon_i = \varepsilon_i c_3$; $c_3 \in \{0, 1\}$
    $j = j + 1$
    if $j \geq j_t$ **then**
      $j_t \Leftarrow$ Iteration threshold to avoid indefinite loop. Increase the value of ε_i compared to the initial value.
      $j = 0$
  $\eta_2 = logical(R_{l,gs} \geq R_1^{th})$
  $i = i + 1$
$H_l^* = d(l, k) \tan(\Theta_{i+1})$

where Θ_i is the solution of i^{th} iteration. The step size function is defined as

$$\varphi_1(\varepsilon_i) = f(\Theta_i) + c_1 \varepsilon_i g_i, \; c_1 \in (0, 1) \;, \tag{4.21}$$

where ε_i is the variable representing the step size in the i^{th} iteration, g_i is the increment direction, and $c_1 \in (0, 1)$ is a constant . Armijo's condition states that the step size ε_i must be chosen such that

$$f(\Theta_i + \varepsilon_i g_i) \geq \varphi_1(\varepsilon_i). \tag{4.22}$$

Armijo's condition ensures sufficient increment in the objective function value. On the other hand, Wolfe's condition states that step size must be chosen such that

$$\varphi_1'(\varepsilon_i) \leq c_2 \varphi_1'(0), \;\; c_2 \in (c_1, 1) \;\; , \tag{4.23}$$

where $\varphi_1'(\varepsilon_i)$ is the rate of increment in the next solution, $\varphi_1'(0)$ is the rate of increment in the current solution, and $c_2 \in (c_1, 1)$ is a constant. Wolfe's condition ensures a lower rate of increment is achieved compared to the fraction of current rate of increment in the given direction.

Considering all of these, the altitude optimization will follow these steps as illustrated in Fig. 4.2. The initial elevation angle will be set as the critical angle of environment respect to the PLoS where The altitude optimization process for the l^{th} UAV is formally stated in Algorithm 5. As per (4.16) and (4.17), altitude optimization can be independently performed for each UAV.

The overall optimization process involving all three subproblems is formally stated in Algorithm 6.

Algorithm 6: Overall optimization

Data: $\mathcal{Q}$
Result: $\mathcal{W}, \Psi, L_{min}$
$L_{min} \Leftarrow$ Minimum number of UAVs required. **begin**
  while $|\Psi| < K$ *and* $L \leq N_{UAV}^{max}$ **do**
    Block-A
      $N_{UAV}^{max} \Leftarrow$ Maximum number of UAVs available
      $n = 0 \Leftarrow$ Iteration index.
      Set G_0 to a positive value
      $g_s(0) = 0$
      while $G_0 > 0$ **do**
        $n = n + 1$
        Execute Algorithm 3 and obtain Ψ_n
        $\Psi_n \Leftarrow$ Optimal UAV-SN association in the n^{th} iteration
        Using Ψ_n execute Algorithm 4 and obtain $\boldsymbol{q_n^*}$
        $\boldsymbol{q_n^*} \Leftarrow$ Optimal 2D position in the n^{th} iteration
        $G_0 = g_s(n) - g_s(n-1)$
        $g_s(n) \Leftarrow g_s$ value returned by algorithm 4 in the n^{th} iteration
      for $l = 1, \ldots, L$ **do**
        Execute Algorithm 5 and obtain H_l^*
    if $|\Psi|$ *Increases* **then**
      Goto **Block-A**
    else if $|\Psi| < K$ **then**
      $L = L + 1$
  $L_{min} = L$;

As we shown in section 4.3.3, altitude optimization can be done independently of others. Therefore, in the overall optimization, we alternatively solve $P1$ and $P2$ until convergence. Then, it will check whether all SNs are served with the required rate and power constraints. If some SNs cannot be served as per the

given QoS constraints, it will add another UAV and repeat $P1$ and $P2$. This will continue until all the SNs are served, or the maximum number of UAVs is reached. After that, the altitude of each UAV will be optimized.

4.3.5 Complexity Analysis

The time complexity of each iteration of modified pattern search is $\mathcal{O}(K)$ since each SN will be accessed one time within a single iteration. Thus, the computation time for 2D positioning will linearly increase with the number of SNs. In naive pattern search, all the users performance will be accessed m times within each iteration where m is the resolution of the pattern search. Therefore, the time complexity of naive pattern search is $\mathcal{O}(m \times K)$. Since m is a constant, the effective time complexity is $\mathcal{O}(K)$. Although the time complexities of the modified PS and the naive PS are similar as per the standard analysis, the actual time taken for each iteration in naive PS is higher than the modified PS since $m \geq 4$ for the 2D search space. The time complexity of the proposed altitude optimization is $\mathcal{O}(1)$, as it does not depend on the number of SNs. On the other hand, the altitude selection approach proposed in [81] has the time complexity of $\mathcal{O}(K)$ as it assess all the SNs in each iterations.

In the worst case scenario, the number of weights Algorithm 3 need to check is less than $K \times L$. This is because in the n^{th} connection phase, we do not need to check the weights of the SNs which are already associated. Therefore, the worst case time complexity of Algorithm 3 can be given as $\mathcal{O}(K \times L)$. However, the worst case time complexity of conventional Gale-Shapely algorithm can be as large as $\mathcal{O}(K \times L^2)$, since it should satisfy mutual priorities.

4.4 Simulation Results and Discussion

This section presents numerical and simulation results to evaluate the proposed algorithms' performance and provide insights for system design. We compare the performance of the proposed scheme with baseline approaches. A square area of $500 \times 500\, m^2$ is considered in numerical simulation. Unless otherwise specified, the parameters used in numerical results are given in Table 4.1.

Table 4.1: Simulation settings

G_1	1×10^{-2}	B_c	1 MHz
$h_{\min}$	20 m	G_{LS}	5×10^{-3}
G_{NS}	2×10^{-3}	N_0	-100 dBm
B_o	1 MHz	α_{LS}	2.0
α_{NS}	2.5	κ	1.5
R_1^{th}	30 Mbps	R_2^{th}	1 Mbps
$P_{u,max}$	10 W	$P_{s,max}$	1 mW
N_{max}	10	N_{UAV}^{max}	15
c_1	0.1	c_2	0.9
c_3	0.6	ϱ	1×10^{-15}
σ, β	4.8800, 0.4290 (Suburban) 9.6117, 0.1581 (Urban) 12.0810, 0.1140 (Dense urban) 24.5960, 0.1248 (High-rise urban)		

First, we study the effectiveness of the modified matching algorithm given in Algorithm 3. Fig. 4.6 illustrates the maximum transmit power requirement achieved through a conventional matching algorithm and our proposed approach in Algorithm 3 for various numbers of SNs. For each number of SNs it is repeated for 10000 random distribution and the results are averaged. Fig. 4.6 shows that the proposed approach does the UAV-SN assignment such that it minimizes the maximum transmit power requirement compared to the conventional matching algorithm proposed in [27]. Although the proposed approach outperforms regardless of the number of SNs, it can be observed that the maximum transmit power shows a zig-zag behavior with the number of SNs. It is related to the total number of resource blocks and the total number of SNs. If both are equal, it should utilize all the UAVs' resource blocks regardless of the worst channel conditions it has for particular SNs. Thus, it results in a higher maximum transmit power requirement. On the other hand, if resource blocks are higher than SNs it has the flexibility of assigning the SN to UAVs, which helps avoid the worst UAV-SN pairing and decreases the maximum transmit power requirement. In this example, the number of resource blocks in a single UAV (N_{max}) is 8. Thus, it shows peaks in maximum transmit power requirement for multiples of 8 in terms of

the number of SNs. Therefore, avoiding the worst UAV-SN assignment is crucial when we consider the fairness among the SNs. Thus, we did a minor modification to Algorithm 3 such that it helps to avoid the worst UAV-SN assignment. The modified algorithm is referred to as Algorithm 3-b.

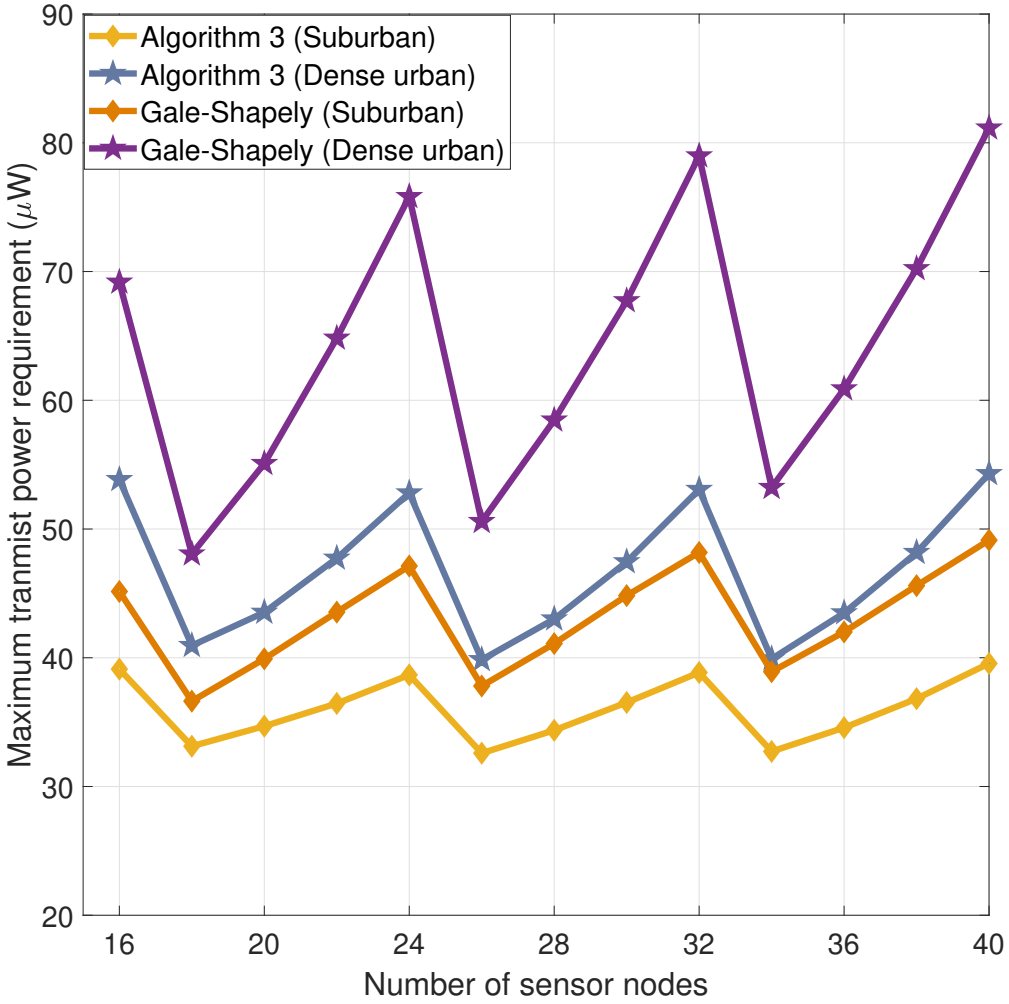

Fig. 4.6: The maximum transmit power required among all the SNs for varying number of SNs. $N_{max} = 8$.

In Algorithm 3, in the n^{th} connection phase, it gives the connection priority as per the weight of SN's n^{th} preferred connection in the ascending order. In Algorithm 3-b, in the n^{th} connection phase, the connection priority is given as per the weight of $(n+1)^{\text{th}}$ preferred connection. Thus, it helps to avoid the worst UAV-SN assignment in the next phase. Fig. 4.7 illustrates the maximum transmit power requirement achieved through Algorithm 3 and Algorithm 3-b for the same simulation setup adopted for the results showed in Fig. 4.6. Fig. 4.7

shows that Algorithm 3-b does the UAV-SN assignment such that it minimizes the maximum transmit power requirement compared to Algorithm 3 and the conventional matching algorithm proposed in [27]. Also, it is observable that Algorithm 3 and Algorithm 3-b gives higher gain when the number of SNs is equal to multiples of the maximum number of SNs a single UAV can serve (N_{max}). In this scenario, it is 8. The results shown in Fig. 4.7 are averaged for 10000 random distribution of SNs for each number of SNs.

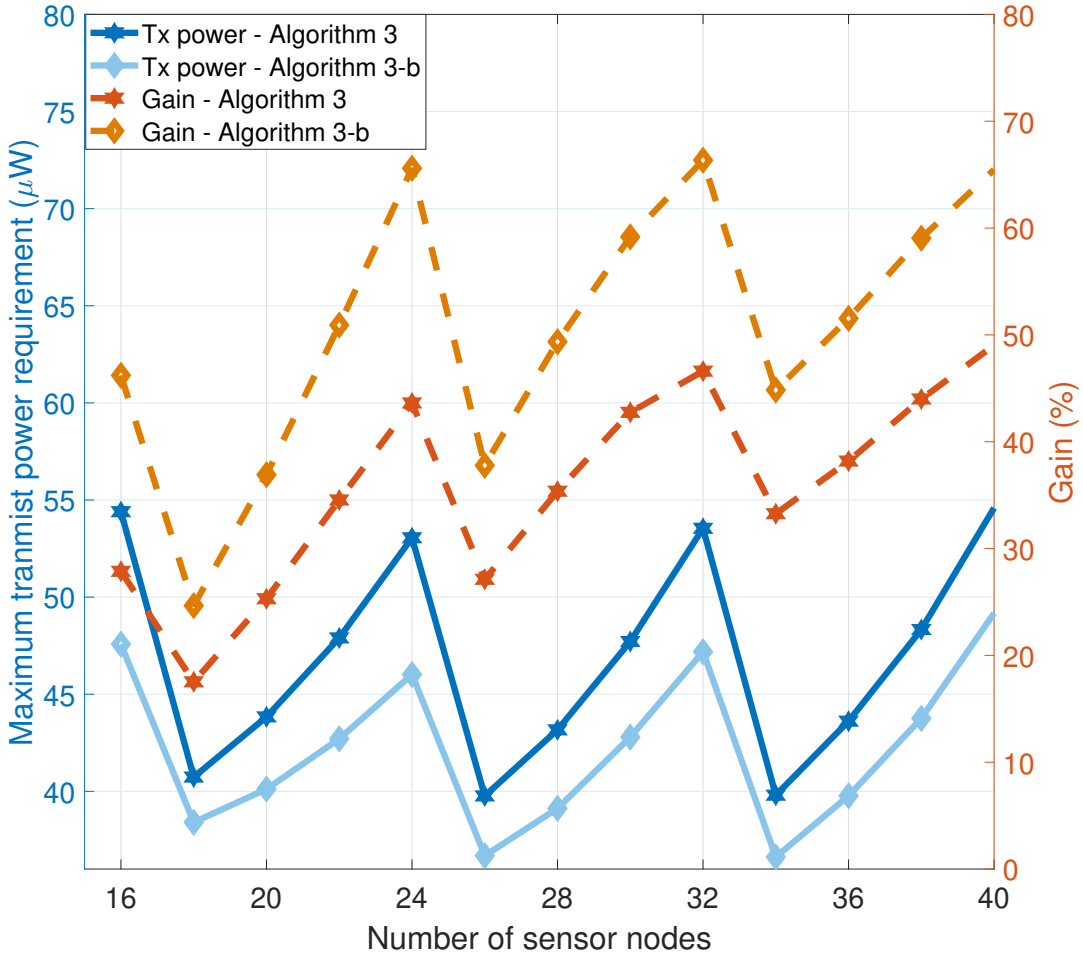

Fig. 4.7: The maximum transmit power required among all the SNs for varying number of SNs and the respective gain achieved compared to conventional Gale-Shapely algorithm in dense urban environment. $N_{max} = 8$.

Although in average Algorithm 3-b performs better, in some instances Algorithm 3 performs better than Algorithm 3-b. Therefore, we compared them as per the frequentist probability. It is calculated through 1 000 000 trials repeated

for various environments for varying number of SNs. Table 4.2 shows the comparison. $P_{(A_3<A_{3-b})}$ refers to the probability where Algorithm 3-b performs better than Algorithm 3. Similarly, $P_{(A_3<A_{3-b})}$ and $P_{(A_3=A_{3-b})}$ refers to the probability lesser and equal performance respectively. It is observable that 92% of the times Algorithm 3-b performs equally or better than Algorithm 3.

Table 4.2: Probabilistic performance comparison of Algorithm 3 and Algorithm 3-b

$P_{(A_3<A_{3-b})}$	$P_{(A_3>A_{3-b})}$	$P_{(A_3=A_{3-b})}$
0.4261	0.0802	0.4937

After that, we analyze the effectiveness of using the PS algorithm for intra-cluster deployment and solving the 3D deployment problem by breaking it into two separate problems. Table 4.3 illustrates the number of iterations it takes to solve the intra-cluster 3D deployment through three different approaches. Approach 1 finds the optimal solution through an exhaustive search that checks every possibility with the given precision. Approach 2 utilizes a 3D naive pattern search to solve the 3D positioning problem. Approach 3 breaks the problem into two subproblems, where it initially optimizes the 2D positioning through the 2D PS algorithm and the altitude is optimized through the 1D PS algorithm. All approaches result in nearly identical performance in terms of maximum transmit power among the SNs. However, Approach 1 requires an exorbitant number of iterations compared to the 3D PS. Also, breaking the 3D positioning into two separate subproblems (Approach 2), results in 2.3 times fewer iterations compared to Approach 1. Moreover, the time complexity of a single iteration in all three approaches is $\mathcal{O}(N_l)$, where N_l is the number of SNs in the respective cluster. Therefore, the number of iterations is a measure of the total time required to solve the problem using each approach.

Fig. 4.8 compares the number of iterations required for convergence with two different approaches in different operating environments. We have compared three approaches, including our proposed approach. Also, we have included Approach 3 for cross-comparison. Approach 4 uses naive pattern search for 2D optimization and exact line search for altitude optimization. The Proposed approach uses a modified pattern search for 2D optimization and a customized inexact line search

Table 4.3: The number of iterations required to solve the 3D deployment problem for a given cluster with $K = 8$.

	Number of iterations		
	Approach 1 (Exhaustive search)	Approach 2 (3D PS)	Approach 3 (2D PS + 1D PS)
Suburban	125000	1812	784
Urban	22250000	5346	3764
Dense urban	3625000	7392	4884
High-rise urban	6625000	11856	7444

for altitude optimization. One can clearly identify the effectiveness of the modified pattern search algorithm and the inexact line search with the Armijo - Wolfe condition used in "Proposed approach". The number of iterations required for the "Proposed approach" is 240% less than Approach 4, which requires a significantly smaller number of iterations among all the other baseline approaches. Therefore, it is clear that the proposed approach significantly simplifies the problem-solving process.

Table 4.4 illustrates the maximum transmit power requirement among the SNs, achieved through Approach 1 and the proposed approach. It can be observed that the proposed approach achieves almost 99% of the performance of

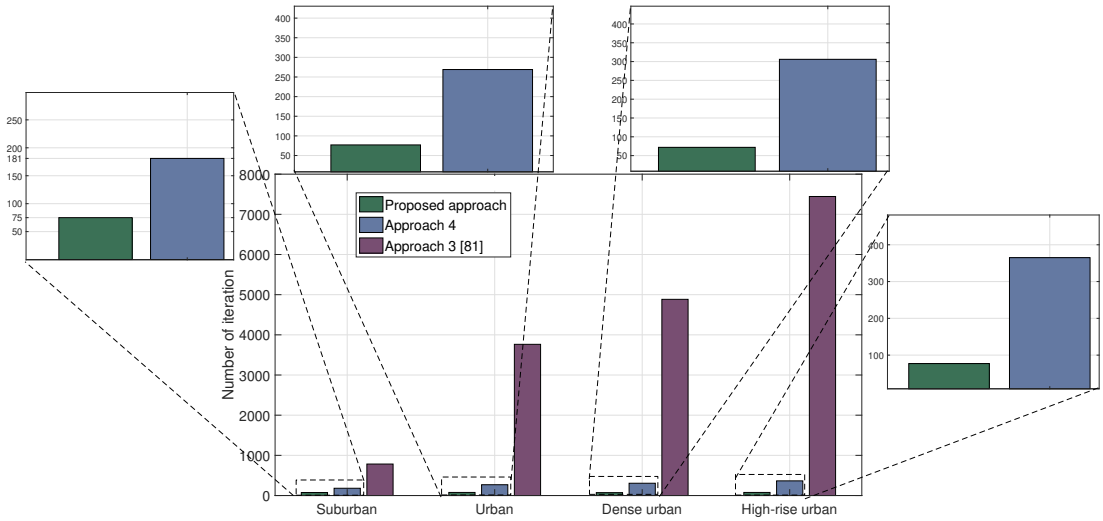

Fig. 4.8: The number of iterations taken to convergence for different approaches in various environment with $K = 8$.

Approach 1, with 1650 times fewer iterations. Therefore, the Proposed approach guarantees near-optimal solutions with very few number of iterations. Moreover, as shown in section 4.3.5, the time complexity involved in each iteration of the proposed approach is less than or equal to the comparative approaches. Given that, the time required to execute one iteration of the proposed approach is less than the respective time required for comparative approaches.

Table 4.4: The maximum transmit power resulted from the exhaustive search and the proposed approach. $K = 8$.

	Approach 1 (Max Tx power)	proposed approach (Max Tx power)	Achievement
Suburban	5.265 μW	5.280 μW	99.72 %
Urban	8.167 μW	8.176 μW	99.89 %
Dense urban	11.763 μW	11.880 μW	99.02 %
High-rise urban	21.764 μW	21.983 μW	99.50 %

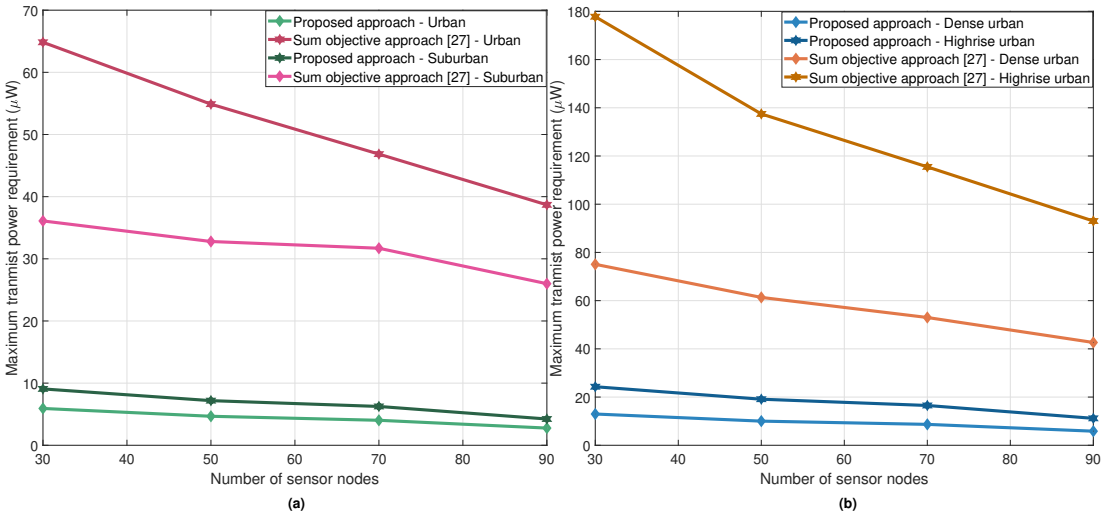

Fig. 4.9: The maximum transmit power required among all the SNs for varying number of of SNs in different environments. (a)- Suburban and Urban; (b)- Dens urban and Highrise urban

Fig. 4.9 illustrates the maximum required transmit power in different environments. We compare the performance of the proposed approach with the approach proposed in [27], referred to as LAYF algorithm. Here, the number of

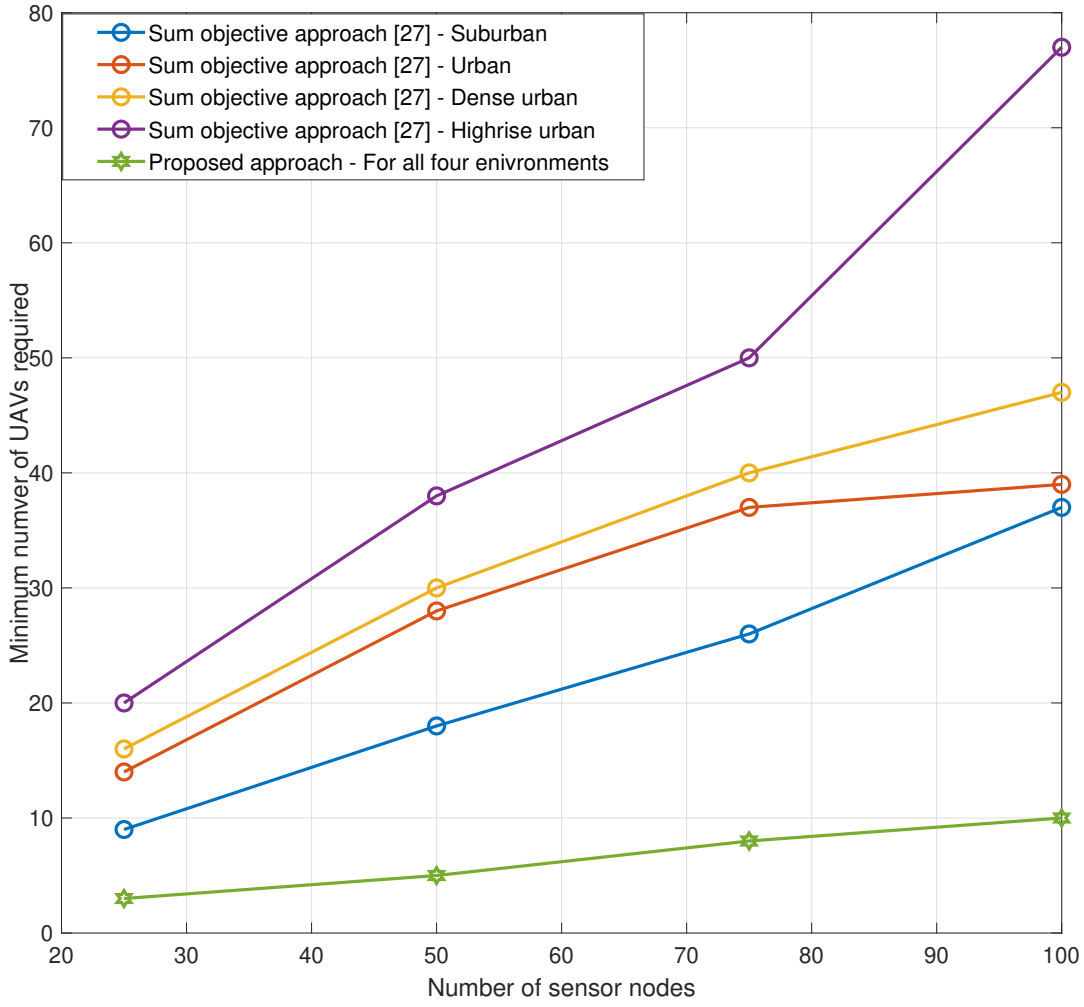

Fig. 4.10: The minimum number of UAVs required to serve all the SNs with varying number of SNs in different environments for $P_0 = 25\,\mu$W.

UAVs is set as per (4.1). The LAYF algorithm is based on accumulated utility, which is a promising approach considering the system's overall performance. However, it does not consider fairness among the users. Fig. 4.9 clearly shows the proposed approach reduces the maximum transmit power requirement by at least 5 fold compared to the LAYF algorithm. It is because the LAYF approach utilizes conventional approaches to solve their subproblems and does not have intra-cluster placement, which is crucial considering the fairness among the SNs. Considering the total transmit power requirement of the system, our proposed approach and LAYF approach both require approximately equal transmit power. In the LAYF approach, both the extremes are there; some SNs require very high transmit power, whereas some require very low power. Thus, the power range

is higher. In contrast, our approach maintains fairness among the SNs, which reduces the range by a huge margin. Since the highs and lows of LAYF cancel out, our approach and LAYF has approximately equal total transmit power requirement.

Also, it can be observed that the maximum required transmit power reduces with the number of SNs, regardless of the approach or the environment. This is because increasing the number of SNs increases the number of UAVs, reducing the distance between the SN and the associated UAV. However, our proposed approach shows a lesser reduction rate since it always tries to maintain the transmit power fairness among the SNs, which reduces the gap between the best and the worst SN. Thus, the maximum required transmit power remains almost constant with the number of SNs. Furthermore, the maximum required transmit power changes with the type of the environment, where it increases in the order, suburban, urban, dense urban, and high-rise urban. This behavior is observed because compared to the suburban environment, UAVs should climb to a higher altitude to establish strong LoS connections in an urban environment, leading to additional pathloss that results in a larger transmit power requirement. The optimal altitude for UAVs increases in the order suburban, urban, dense urban and high-rise urban.

In this work, we have not considered the energy requirement of the UAV movement, as our focus is on the energy efficiency of the SNs. However, the proposed approach will consume less energy for UAV movements, as the UAVs can directly fly to the position identified through the solution, without any sequential movements, as the final UAV position is determined through a centralized approach that utilizes only the SN locations, channel statistics, and environmental parameters. Moreover, centralized and distributed (LAYF) both the approaches should maintain minimum channel quality between the central station for control operation and data forwarding. Given that, centralized approach does not require additional maneuvering energy to forward the information to the central station compared to the distributed approach. Therefore, the centralized approach can significantly reduce the energy consumption of UAV movements compared to a distributed solution, where UAVs have to adjust their locations iteratively [6].

Fig. 4.10 illustrates the minimum number of UAVs required to serve all the SNs while satisfying the maximum power and minimum data rate constraints.

It can be observed that our proposed approach requires fewer number of UAVs compared to the LAYF approach. Since the LAYF algorithm does not include transmit power fairness, a large number of UAVs are required to satisfy the minimum QoS requirements. This highlights the importance of considering transmit power fairness among the SNs. Moreover, the proposed approach requires the same number of UAVs regardless of the environment, as it can achieve a much higher data rate than the threshold data rate with the given constraints in all the environments.

4.5 Conclusion

This chapter investigated the problem of deploying multiple UAVs to collect data from a WSN, considering the transmit power fairness among the SNs. A novel algorithm was proposed by modifying the existing algorithms to ensure fairness in the WSN. The multi-UAV deployment problem was divided into three subproblems to reduce the complexity involved in joint optimization. The three subproblems are UAV-SN association, 2D positioning of the UAVs and the altitude optimization of the UAVs. First, the UAV-SN association is addressed using a customized Gale–Shapley algorithm. Second, the 2D positions of the UAVs are optimized using a modified pattern search algorithm. Third, the altitude of the UAVs are optimized through a customized inexact line search algorithm. Finally, we have proposed the combined optimization algorithm that integrates altogether and provides a single solution. The numerical results confirm the effectiveness of breaking the 3D deployment problem into two subproblems, which reduces the required number of iterations by 2.3 times compared to solving as a single problem. Also, it illustrates the performance improvement of our customized approach in terms of the number of iterations compared to the baseline approaches. It takes 1000 % and 240 % times fewer number of iterations compared to Approach 3 and Approach 4, respectively. Moreover, we have compared the performance of the proposed approach in terms of the maximum transmit power requirement with the baseline approach, which illustrates that the proposed approach consumes 4 times less maximum transmit power. Also, the minimum number of UAVs required to serve all the SNs through the proposed approach is at least 4 times less compared to the baseline approach.

Future Directions

One of the major features of future wireless communication is providing uninterrupted, reliable coverage services. UAVs can be deployed in various wireless systems to accommodate the aforementioned requirement. In this content, many issues appear to be worthwhile for future research. Our work is based on readily available requirements/demands. Future work can focus on demand prediction and pre-deployment, which help increase energy efficiency and other orchestration of the network. Moreover, we can study the user assignment policies given the nature of the distribution, the spatiality of the preference weight matrix and other system characteristics. Future wireless communication is more focused on increasing the average rate rather than further increasing the peak rate. Thus, UAV-assisted cell-free communication also would be a timely topic to analyze.

Bibliography

[1] M. Mozaffari, W. Saad, M. Bennis, Y. -H. Nam and M. Debbah, "A Tutorial on UAVs for Wireless Networks: Applications, Challenges, and Open Problems," *IEEE Communications Surveys & Tutorials*, vol. 21, no. 3, pp. 2334-2360, Mar. 2019.

[2] A. Sharma, P. Vanjani, N. Paliwal, C. M. W. Basnayaka, D. N. Jayakody, H.-C. Wang, and P. Muthuchidambaranathan, "Communication and networking technologies for UAVs: A survey," *Journal of Network and Computer Applications*, vol. 168, p. 102739, Oct. 2020.

[3] K. L. Cook, "The silent force multiplier: the history and role of UAVs in warfare," in *Proc. IEEE Aerospace Conference*, Mar. 2007, pp. 1–7.

[4] C. She et al., "A Tutorial on Ultrareliable and Low-Latency Communications in 6G: Integrating Domain Knowledge Into Deep Learning," in *Proceedings of the IEEE*, vol. 109, no. 3, pp. 204-246, Mar. 2021,

[5] P. Popovski, K. F. Trillingsgaard, O. Simeone and G. Durisi, "5G Wireless Network Slicing for eMBB, URLLC, and mMTC: A Communication-Theoretic View," *IEEE Access*, vol. 6, pp. 55765-55779, Sep. 2018.

[6] H. Hydher, D. N. K. Jayakody, K. T. Hemachandra, and T. Samarasinghe, "Intelligent UAV deployment for a disaster-resilient wireless network," *Sensors*, vol. 20, no. 21, p. 6140, Oct 2020.

[7] D. N. K. Jayakody, T. D. P. Perera, A. Ghrayeb and M. O. Hasna, "Self-Energized UAV-Assisted Scheme for Cooperative Wireless Relay Networks," *IEEE Transactions on Vehicular Technology*, vol. 69, no. 1, pp. 578-592, Jan. 2020.

[8] N. Zhao et al., "UAV-Assisted Emergency Networks in Disasters," *IEEE Wireless Communications*, vol. 26, no. 1, pp. 45-51, Feb. 2019.

[9] D. Orfanus, E. P. de Freitas and F. Eliassen, "Self-Organization as a Supporting Paradigm for Military UAV Relay Networks," *IEEE Communications Letters*, vol. 20, no. 4, pp. 804-807, Apr. 2016,

[10] C. Dragana, G. Stamatescu, L. Ichim and D. Popescu, "Interlinking unmanned aerial vehicles with wireless sensor networks for improved large area monitoring," in *Proc. 4th International Conference on Control, Decision and Information Technologies (CoDIT)*, 2017, pp. 0359-0364,

[11] S. Kahveci, "Some cooperative relaying techniques for wireless communication systems," in *Proc. 22nd Signal Processing and Communications Applications Conference (SIU)*, 2014, pp. 1690-1693, doi: 10.1109/SIU.2014.6830573.

[12] X. Lin, W. Mei and R. Zhang, "A New Store-Then-Amplify-and-Forward Protocol for UAV Mobile Relaying," *IEEE Wireless Communications Letters*, vol. 9, no. 5, pp. 591-595, May 2020.

[13] W. Huang, J. Peng and H. Zhang, "User-Centric Intelligent UAV Swarm Networks: Performance Analysis and Design Insight," *IEEE Access*, vol. 7, pp. 181469-181478, Dec. 2019.

[14] A. Al-Hourani, S. Kandeepan and S. Lardner, "Optimal LAP Altitude for Maximum Coverage," *IEEE Wireless Communications Letters*, vol. 3, no. 6, pp. 569-572, Dec. 2014.

[15] M. Mozaffari, W. Saad, M. Bennis and M. Debbah, "Efficient Deployment of Multiple Unmanned Aerial Vehicles for Optimal Wireless Coverage," *IEEE Communications Letters*, vol. 20, no. 8, pp. 1647-1650, Aug. 2016.

[16] M. Alzenad, A. El-Keyi, F. Lagum and H. Yanikomeroglu, "3-D Placement of an Unmanned Aerial Vehicle Base Station (UAV-BS) for Energy-Efficient Maximal Coverage," *in IEEE Wireless Communications Letters*, vol. 6, no. 4, pp. 434-437, Aug. 2017.

[17] Xukai Zhong, "Deploying UAV Base Stations in Communication Network Using Machine Learning," Master of Engineering dissertation, Department

of Electrical and Computer Engineering., Simon Fraser University., Burnaby, Canada, 2017. Accessed on: January 10, 2019. [Online]. Available: https://dspace.library.uvic.ca/handle/1828/11405.

[18] M. J. Farooq and Q. Zhu, "A Multi-Layer Feedback System Approach to Resilient Connectivity of Remotely Deployed Mobile Internet of Things," *IEEE Transactions on Cognitive Communications and Networking*, vol. 4, no. 2, pp. 422-432, June 2018.

[19] F. Jiang and A. L. Swindlehurst, "Optimization of UAV Heading for the Ground-to-Air Uplink," *IEEE Journal on Selected Areas in Communications*, vol. 30, no. 5, pp. 993-1005, June 2012.

[20] J. Chen and D. Gesbert, "Optimal positioning of flying relays for wireless networks: A LOS map approach," in *Proc. IEEE International Conference on Communications (ICC)*, Paris, 2017, pp. 1-6.

[21] Y. Li, G. Feng, M. Ghasemiahmadi and L. Cai, "Power Allocation and 3-D Placement for Floating Relay Supporting Indoor Communications," *IEEE Transactions on Mobile Computing*, vol. 18, no. 3, pp. 618-631, Mar. 2019.

[22] H. Shakhatreh, A. Khreishah, A. Alsarhan, I. Khalil, A. Sawalmeh and N. S. Othman, "Efficient 3D placement of a UAV using particle swarm optimization," in *Proc. 8th International Conference on Information and Communication Systems (ICICS)*, Irbid, 2017, pp. 258-263.

[23] J. Sánchez-García, D.G. Reina, S.L. Toral, A distributed PSO-based exploration algorithm for a UAV network assisting a disaster scenario, *Future Generation Computer Systems*, Volume 90, Pages 129-148, 2019.

[24] D.G. Reina, T. Camp, A. Munjal, S.L. Toral, Evolutionary deployment and local search-based movements of 0th responders in disaster scenarios, *Future Generation Computer Systems*, Volume 88, Pages 61-78, 2018.

[25] A. Chattopadhyay, A. Ghosh and A. Kumar, "Asynchronous Stochastic Approximation Based Learning Algorithms for As-You-Go Deployment of Wireless Relay Networks Along a Line," *IEEE Transactions on Mobile Computing*, vol. 17, no. 5, pp. 1004-1018, 1 May 2018.

[26] J. Li and Y. Han, "Optimal Resource Allocation for Packet Delay Minimization in Multi-Layer UAV Networks," *IEEE Communications Letters*, vol. 21, no. 3, pp. 580-583, Mar. 2017.

[27] H. El Hammouti, M. Benjillali, B. Shihada and M. Alouini, "Learn-As-You-Fly: A Distributed Algorithm for Joint 3D Placement and User Association in Multi-UAVs Networks," *IEEE Transactions on Wireless Communications*, vol. 18, no. 12, pp. 5831-5844, Dec. 2019.

[28] B. Duo, Q. Wu, X. Yuan and R. Zhang, "Energy Efficiency Maximization for Full-Duplex UAV Secrecy Communication," *IEEE Transactions on Vehicular Technology*, vol. 69, no. 4, pp. 4590-4595, Apr. 2020.

[29] S. Karimi-Bidhendi, J. Guo and H. Jafarkhani, "Energy-Efficient Node Deployment in Heterogeneous Two-Tier Wireless Sensor Networks With Limited Communication Range," *IEEE Transactions on Wireless Communications*, vol. 20, no. 1, pp. 40-55, Jan. 2021.

[30] Y. Cai, Z. Wei, R. Li, D. W. Kwan Ng and J. Yuan, "Energy-Efficient Resource Allocation for Secure UAV Communication Systems," in *Proc. IEEE Wireless Communications and Networking Conference (WCNC)*, Marrakesh, Morocco, 2019, pp. 1-8.

[31] Y. Wu, W. Yang, X. Guan and Q. Wu, "Energy-Efficient Trajectory Design for UAV-Enabled Communication Under Malicious Jamming," *IEEE Wireless Communications Letters*, vol. 10, no. 2, pp. 206-210, Feb. 2021.

[32] L. Wang and S. Zhou, "Energy-Efficient UAV Deployment with Flexible Functional Split Selection," in *Proc. IEEE 19th International Workshop on Signal Processing Advances in Wireless Communications (SPAWC)*, Kalamata, Greece, 2018, pp. 1-5.

[33] S. Ahmed, M. Z. Chowdhury and Y. M. Jang, "Energy-Efficient UAV Relaying Communications to Serve Ground Nodes," *IEEE Communications Letters*, vol. 24, no. 4, pp. 849-852, Apr. 2020.

[34] V. Mayor, R. Estepa, A. Estepa, and G. Madinabeitia, "Energy-Efficient UAVs Deployment for QoS-Guaranteed VoWiFi Service," *Sensors*, 20(16), p.4455 2020.

[35] S. Ahmed, M. Z. Chowdhury and Y. M. Jang, "Energy-Efficient UAV-to-User Scheduling to Maximize Throughput in Wireless Networks," *IEEE Access*, vol. 8, pp. 21215-21225, 2020.

[36] A. Akarsu and T. Girici, "Fairness aware multiple drone base station deployment," *IET Communications*, 12(4), pp.425-431, 2018.

[37] Yuanxin Cai, Zhiqiang Wei, Ruide Li, Derrick Wing Kwan Ng, Jinhong Yuan "Joint Trajectory and Resource Allocation Design for Energy-Efficient Secure UAV Communication Systems" available online arXiv:2003.07028, Mar 2020

[38] M. Mozaffari, W. Saad, M. Bennis and M. Debbah, "Mobile Internet of Things: Can UAVs Provide an Energy-Efficient Mobile Architecture?," in *Proc. IEEE Global Communications Conference (GLOBECOM)*, Washington, DC, USA, 2016, pp. 1-6.

[39] H. Hu et al., "Optimization of Energy Utilization in Cognitive UAV Systems," *IEEE Sensors Journal*, vol. 21, no. 3, pp. 3933-3943, 1 Feb.1, 2021.

[40] E. Koyuncu, "Power-Efficient Deployment of UAVs as Relays,"in *Proc. IEEE 19th International Workshop on Signal Processing Advances in Wireless Communications (SPAWC)*, Kalamata, Greece, 2018, pp. 1-5.

[41] L. Xiao, Y. Xu, D. Yang and Y. Zeng, "Secrecy Energy Efficiency Maximization for UAV-Enabled Mobile Relaying," *IEEE Transactions on Green Communications and Networking*, vol. 4, no. 1, pp. 180-193, Mar. 2020.

[42] M. Hua, L. Yang, Q. Wu and A. L. Swindlehurst, "3D UAV Trajectory and Communication Design for Simultaneous Uplink and Downlink Transmission," *IEEE Transactions on Communications*, vol. 68, no. 9, pp. 5908-5923, Sept. 2020.

[43] Weidong Mei, Qingqing Wu, Rui Zhang "Cellular-Connected UAV: Uplink Association, Power Control and Interference Coordination" available online arXiv:1807.08218, Jul 2018.

[44] D. Yang, Q. Wu, Y. Zeng and R. Zhang, "Energy Tradeoff in Ground-to-UAV Communication via Trajectory Design," *IEEE Transactions on Vehicular Technology*, vol. 67, no. 7, pp. 6721-6726, July 2018.

[45] A. Rahmati, S. Hosseinalipour, Y. Yapıcı, İ. Güvenç, H. Dai and A. Bhuyan, "Energy-Efficient Beamforming and Power Control for Uplink NOMA in mmWave UAV Networks," in *Proc.GLOBECOM IEEE Global Communications Conference*, Taipei, Taiwan, 2020, pp. 1-6.

[46] H. Huang and A. V. Savkin, "A Method for Optimized Deployment of Unmanned Aerial Vehicles for Maximum Coverage and Minimum Interference in Cellular Networks," *IEEE Transactions on Industrial Informatics*, vol. 15, no. 5, pp. 2638-2647, May 2019.

[47] N. Sharma, M. Magarini, D. N. K. Jayakody, V. Sharma and J. Li, "On-Demand Ultra-Dense Cloud Drone Networks: Opportunities, Challenges and Benefits," *IEEE Communications Magazine*, vol. 56, no. 8, pp. 85-91, August 2018.

[48] H. Zhao, H. Liu, Y. -W. Leung and X. Chu, "Self-Adaptive Collective Motion of Swarm Robots," *IEEE Transactions on Automation Science and Engineering*, vol. 15, no. 4, pp. 1533-1545, Oct. 2018.

[49] M. Delight, S. Ramakrishnan, T. Zambrano and T. MacCready, "Developing robotic swarms for ocean surface mapping," in *Proc. IEEE International Conference on Robotics and Automation (ICRA)*, 2016, pp. 5309-5315.

[50] S. Moon, K. Yang, S. K. Gan and D. H. Shim, "Decentralized information-theoretic task assignment for searching and tracking of moving targets," in *Proc. International Conference on Unmanned Aircraft Systems (ICUAS)*, 2015, pp. 1031-1036.

[51] H. Zhao, H. Wang, W. Wu and J. Wei, "Deployment Algorithms for UAV Airborne Networks Toward On-Demand Coverage," *IEEE Journal on Selected Areas in Communications*, vol. 36, no. 9, pp. 2015-2031, Sept. 2018.

[52] Z. Wang, L. Duan and R. Zhang, "Adaptive Deployment for UAV-Aided Communication Networks," *IEEE Transactions on Wireless Communications*, vol. 18, no. 9, pp. 4531-4543, Sept. 2019.

[53] E. Kalantari, I. Bor-Yaliniz, A. Yongacoglu and H. Yanikomeroglu, "User association and bandwidth allocation for terrestrial and aerial base stations

with backhaul considerations," in *Proc. IEEE 28th Annual International Symposium on Personal, Indoor, and Mobile Radio Communications (PIMRC)*, 2017, pp. 1-6.

[54] X. Zhang and L. Duan, "Fast Deployment of UAV Networks for Optimal Wireless Coverage," *IEEE Transactions on Mobile Computing*, vol. 18, no. 3, pp. 588-601, 1 March 2019.

[55] M. Chen, M. Mozaffari, W. Saad, C. Yin, M. Debbah and C. S. Hong, "Caching in the Sky: Proactive Deployment of Cache-Enabled Unmanned Aerial Vehicles for Optimized Quality-of-Experience," *IEEE Journal on Selected Areas in Communications*, vol. 35, no. 5, pp. 1046-1061, May 2017.

[56] R. Dutta, L. Sun and D. Pack, "A Decentralized Formation and Network Connectivity Tracking Controller for Multiple Unmanned Systems," *IEEE Transactions on Control Systems Technology*, vol. 26, no. 6, pp. 2206-2213, Nov. 2018.

[57] R. Olfati-Saber and P. Jalalkamali, "Coupled Distributed Estimation and Control for Mobile Sensor Networks," *IEEE Transactions on Automatic Control*, vol. 57, no. 10, pp. 2609-2614, Oct. 2012.

[58] I. Mahjri, A. Dhraief, A. Belghith and A. S. AlMogren, "SLIDE: A Straight Line Conflict Detection and Alerting Algorithm for Multiple Unmanned Aerial Vehicles," *IEEE Transactions on Mobile Computing*, vol. 17, no. 5, pp. 1190-1203, 1 May 2018.

[59] S. Panic, T. D. P. Perera, D. N. K. Jayakody, C. Stefanovic and B. Prlincevic, "UAV-assited Wireless Powered Sensor Network over Rician Shadowed Fading Channels," in *Proc. IEEE International Conference on Microwaves, Antennas, Communications and Electronic Systems (COMCAS)*, 2019, pp. 1-5.

[60] J. Kennedy and R. Eberhart, "Particle swarm optimization," in *Proc. ICNN'95 - International Conference on Neural Networks*, 1995, pp. 1942-1948 vol.4.

[61] E. Kalantari, H. Yanikomeroglu and A. Yongacoglu, "On the Number and 3D Placement of Drone Base Stations in Wireless Cellular Networks," in *Proc. IEEE 84th Vehicular Technology Conference (VTC-Fall)*, 2016, pp. 1-6.

[62] M. Mozaffari, W. Saad, M. Bennis and M. Debbah, "Unmanned Aerial Vehicle With Underlaid Device-to-Device Communications: Performance and Tradeoffs," *IEEE Transactions on Wireless Communications*, vol. 15, no. 6, pp. 3949-3963, June 2016.

[63] Y. Sun, Z. Ding and X. Dai, "A User-Centric Cooperative Scheme for UAV-Assisted Wireless Networks in Malfunction Areas," *IEEE Transactions on Communications*, vol. 67, no. 12, pp. 8786-8800, Dec. 2019.

[64] H. Bayerlein, M. Theile, M. Caccamo and D. Gesbert, "UAV path planning for wireless data harvesting: A deep reinforcement learning approach", in *Proc. IEEE Global Commun. Conf. (GLOBECOM)*, pp. 1-6, 2020.

[65] C. -L. Hu, S. -Z. Huang, Z. Zhang and L. Hui, "Energy-Balanced Optimization on Flying Ferry Placement for Data Gathering in Wireless Sensor Networks," *IEEE Access*, vol. 9, pp. 70906-70923, May 2021.

[66] J. Li et al., "Joint Optimization on Trajectory, Altitude, Velocity, and Link Scheduling for Minimum Mission Time in UAV-Aided Data Collection," *IEEE Internet of Things Journal*, vol. 7, no. 2, pp. 1464-1475, Feb. 2020.

[67] Y. Wang, Z. Hu, X. Wen, Z. Lu, and J. Miao, "Minimizing data collection time with collaborative UAVs in wireless sensor networks," *IEEE Access*, vol. 8, pp. 98 659–98 669, May 2020.

[68] S. Alfattani, W. Jaafar, H. Yanikomeroglu, and A. Yongacoglu, "Multiuav data collection framework for wireless sensor networks," in *Proc. IEEE Glob. Commun. Conf.*, 2019, pp. 1–6.

[69] O. Ghdiri, W. Jaafar, S. Alfattani, J. B. Abderrazak and H. Yanikomeroglu, "Energy-Efficient Multi-UAV Data Collection for IoT Networks with Time Deadlines," in *Proc. GLOBECOM 2020 - 2020 IEEE Global Communications Conference*, 2020, pp. 1-6.

[70] C. Zhou et al., "Deep RL-based trajectory planning for AOI minimization in UAV-assisted IoT," in *Proc. IEEE 11th Int. Conf. Wireless Commun. Signal Process*, 2019, pp. 1–6.

[71] C. M. W. Basnayaka, D. N. K. Jayakody and Z. Chang, "Age of Information Based URLLC-enabled UAV Wireless Communications System," *IEEE Internet of Things Journal*, doi: 10.1109/JIOT.2021.3123431.

[72] O. Bouhamed, H. Ghazzai, H. Besbes and Y. Massoud, "A UAV-Assisted Data Collection for Wireless Sensor Networks: Autonomous Navigation and Scheduling," *IEEE Access*, vol. 8, pp. 110446-110460, Jun. 2020.

[73] M. Ibrahim and H. Arslan, "Air-Ground Doppler-delay spread spectrum for dense scattering environments," in *Proc. MILCOM 2015 - 2015 IEEE Military Communications Conference*, 2015, pp. 1661-1666.

[74] K. Daniel, M. Putzke, B. Dusza and C. Wietfeld, "Three dimensional channel characterization for low altitude aerial vehicles," in *Proc. 2010 7th International Symposium on Wireless Communication Systems*, 2010, pp. 756-760.

[75] D. W. Matolak and R. Sun, "Air–Ground Channel Characterization for Unmanned Aircraft Systems—Part I: Methods, Measurements, and Models for Over-Water Settings," *IEEE Transactions on Vehicular Technology*, vol. 66, no. 1, pp. 26-44, Jan. 2017.

[76] R. Amorim, H. Nguyen, P. Mogensen, I. Z. Kovács, J. Wigard and T. B. Sørensen, "Radio Channel Modeling for UAV Communication Over Cellular Networks," *IEEE Wireless Communications Letters*, vol. 6, no. 4, pp. 514-517, Aug. 2017.

[77] Y. Liu, S. Xie and Y. Zhang, "Cooperative Offloading and Resource Management for UAV-Enabled Mobile Edge Computing in Power IoT System," *IEEE Transactions on Vehicular Technology*, vol. 69, no. 10, pp. 12229-12239, Oct. 2020.

[78] F. Zhou, Y. Wu, R. Q. Hu and Y. Qian, "Computation Rate Maximization in UAV-Enabled Wireless-Powered Mobile-Edge Computing Systems," *IEEE Journal on Selected Areas in Communications*, vol. 36, no. 9, pp. 1927-1941, Sept. 2018.

[79] Z. Hu, Z. Zheng, L. Song, T. Wang and X. Li, "UAV Offloading: Spectrum Trading Contract Design for UAV-Assisted Cellular Networks," *IEEE Transactions on Wireless Communications*, vol. 17, no. 9, pp. 6093-6107, Sept. 2018.

[80] 'Propagation data and prediction methods for the design of terrestrial broadband millimetric radio access systems', Geneva, Switzerland, Rec. P.1410-2, 2003, P Series, Radiowave Propagation.

[81] A. Omran, L. Sboui, M. Kadoch, Z. Chang, J. Lu and R. Liu, "3D Deployment of Multiple UAVs for Emergent On-Demand Offloading," in *Proc. 2020 International Wireless Communications and Mobile Computing (IWCMC)*, 2020, pp. 692-696.

[82] H. Hydher, D.N.K. Jayakody, S.Panic, "Maximizing the latency fairness in UAV-assisted MEC system," *IET Intell. Transp. Syst.*, 1–11, 2021.

[83] J. Liu and Q. Liu, "Speed and Resource Optimization of BFGS Quasi-Newton Implementation on FPGA Using Inexact Line Search Method for Neural Network Training," in *Proc. International Conference on Field-Programmable Technology (FPT)*, 2018.

[84] J. Zhang, "On the Non-monotone Armijo-type Line Search Algorithm," in *Proc. Third International Conference on Information and Computing*, 2010, pp. 308-311.

[85] N. Krejić and N. Krklec, "Line search methods with variable sample size for unconstrained optimization," *Journal of Computational and Applied Mathematics*, Volume 245, 2013, Pages 213-231, ISSN 0377-0427.

[86] S. Sharma, Y. Shi, Y. T. Hou and S. Kompella, "An Optimal Algorithm for Relay Node Assignment in Cooperative Ad Hoc Networks," *IEEE/ACM Transactions on Networking*, vol. 19, no. 3, pp. 879-892, June 2011.

[87] S. Chowdhury, "Matching theory for cognitive radio networks: An overview", *ICT Express*, vol. 5, no. 1, pp. 12-15, 2019.